Am J Physiol Cell Physiol 282: C434–C450, 2002.
First published October 31, 2001; 10.1152/ajpcell.00240.2001.

Vasopressin-mediated mitogenic signaling in intestinal epithelial cells

TERENCE CHIU, STEVEN S. WU, CHINTDA SANTISKULVONG, PISIT TANGKIJVANICH, HAL F. YEE, JR., AND ENRIQUE ROZENGURT
Department of Medicine, School of Medicine, and Molecular Biology Institute, University of California, Los Angeles, California 90095

Received 10 August 2001; accepted in final form 29 October 2001

Chiu, Terence, Steven S. Wu, Chintda Santiskulvong, Pisit Tangkijvanich, Hal F. Yee, Jr., and Enrique Rozengurt. Vasopressin-mediated mitogenic signaling in intestinal epithelial cells. *Am J Physiol Cell Physiol* 282: C434–C450, 2002. First published October 31, 2001; 10.1152/ajpcell.00240.2001.—The role of G protein-coupled receptors and their ligands in intestinal epithelial cell signaling and proliferation is poorly understood. Here, we demonstrate that arginine vasopressin (AVP) induces multiple intracellular signal transduction pathways in rat intestinal epithelial IEC-18 cells via a V_{1A} receptor. Addition of AVP to these cells induces a rapid and transient increase in cytosolic Ca^{2+} concentration and promotes protein kinase D (PKD) activation through a protein kinase C (PKC)-dependent pathway, as revealed by in vitro kinase assays and immunoblotting with an antibody that recognizes autophosphorylated PKD at Ser^{916}. AVP also stimulates the tyrosine phosphorylation of the nonreceptor tyrosine kinase proline-rich tyrosine kinase 2 (Pyk2) and promotes Src family kinase phosphorylation at Tyr^{418}, indicative of Src activation. AVP induces extracellular signal-related kinase (ERK)-1 ($p44^{mapk}$) and ERK-2 ($p42^{mapk}$) activation, a response prevented by treatment with mitogen-activated protein kinase kinase (MEK) inhibitors (PD-98059 and U-0126), specific PKC inhibitors (GF-I and Ro-31-8220), depletion of Ca^{2+} (EGTA and thapsigargin), selective epidermal growth factor receptor (EGFR) tyrosine kinase inhibitors (tyrphostin AG-1478, compound 56), or the selective Src family kinase inhibitor PP-2. Furthermore, AVP acts as a potent growth factor for IEC-18 cells, inducing DNA synthesis and cell proliferation through ERK-, Ca^{2+}-, PKC-, EGFR tyrosine kinase-, and Src-dependent pathways.

arginine vasopressin; protein kinase D; protein kinase C; Src; proline-rich tyrosine kinase 2; intestinal epithelial proliferation

THE SEQUENTIAL PROLIFERATION, lineage-specific differentiation, migration, and cell death of epithelial cells of the intestinal mucosa is a tightly regulated process that is modulated by a broad spectrum of regulatory peptides (8, 36, 70). The nontransformed IEC-6 and IEC-18 cells, derived from rat small intestinal crypt (56), have provided an in vitro model to examine intestinal epithelial cell migration, differentiation, and proliferation (16, 27, 58, 70). Previous studies demonstrated that the proliferation and migration of these intestinal epithelial cells is regulated by a variety of polypeptide growth factors, including epidermal growth factor (EGF), insulin-like growth factor I, and hepatocyte growth factor, which act via single-pass transmembrane tyrosine kinase receptors (3, 17, 51). Neuropeptides and vasoactive peptides that signal through G protein-coupled receptors (GPCRs), characterized by seven-transmembrane helices, also act as potent cellular growth factors for a variety of cell types (63, 64, 66, 67). However, the role of GPCRs and their ligands in intestinal epithelial cell signaling and proliferation remains poorly understood.

The neurohypophysial nonapeptide arginine vasopressin (AVP), also known as antidiuretic hormone, is traditionally recognized for its role as a vasoconstrictor hormone acting on vascular smooth muscle cells and its antidiuretic effect via the renal collecting system. In addition to its function in the regulation of body fluid osmolality, vascular tone, and blood pressure, AVP acts as a growth-promoting factor for a variety of cell types including fibroblasts, hepatocytes, vascular smooth muscle cells, and small cell lung carcinoma (62, 68, 74, 77). AVP is known to exert its biological effects through binding to three AVP receptor subtypes, V_{1A}, V_{1B}, and V_2 receptors, which are members of the GPCR superfamily (6). V_{1A} and V_{1B} receptors induce phospholipase C (PLC)-mediated hydrolysis of membrane phosphoinositides leading to the generation of two second messengers: inositol 1,4,5-trisphosphate [$Ins(1,4,5)P_3$], which stimulates Ca^{2+} mobilization from intracellular stores and diacylglycerol (DAG), which activates the classic and novel isoforms of the protein kinase C (PKC) family. V_{1A} receptor activation also leads to rapid stimulation of nonreceptor tyrosine kinases including Src family kinases and focal adhesion kinase (60, 61) and mitogen-activated protein (MAP) kinase (MAPK) cascades (28). V_2 receptors, which are predominantly found in the renal collecting system, induce G_s-mediated adenylate cyclase stimulation, leading to increased cAMP synthesis (6).

Address for reprint requests and other correspondence: E. Rozengurt, 900 Veteran Ave., Warren Hall, Rm. 11–124, Dept. of Medicine, UCLA School of Medicine, Los Angeles, CA 90095-1786 (E-mail: erozengurt@mednet.ucla.edu).

The costs of publication of this article were defrayed in part by the payment of page charges. The article must therefore be hereby marked "*advertisement*" in accordance with 18 U.S.C. Section 1734 solely to indicate this fact.

In the human gastrointestinal tract, earlier studies demonstrated the presence of vasopressin in crypt cells of the stomach and small intestine and in mononuclear cells within the lamina propria and submucosa as revealed by immunohistochemical examination (24). More recently, AVP-containing cells have been reported to be present in rat small and large intestines (35), as well as in a subpopulation of enteric neurons in the submucosal and myenteric plexuses of the canine colon (82). AVP has been shown to mediate electrolyte and water transport in the colon (71). To date, there are no studies concerning AVP-stimulated signaling, including effects on protein kinase cascades and cell proliferation, in cultures of intestinal epithelial cells.

In the present study we demonstrate, for the first time, that AVP potently induces multiple intracellular signal transduction pathways in nontransformed rat intestinal epithelial IEC-18 cells via a V_{1A} receptor subtype. Addition of AVP to these cells induces a rapid elevation in the intracellular concentration of Ca^{2+} ($[Ca^{2+}]_i$) and promotes protein kinase D (PKD) activation through a PKC-dependent pathway. Furthermore, AVP stimulates the nonreceptor tyrosine kinases proline-rich tyrosine kinase 2 (Pyk2) and Src and induces activation of the extracellular signal-regulated kinases (ERKs) ERK-1 ($p44^{mapk}$) and ERK-2 ($p42^{mapk}$), through $[Ca^{2+}]_i$-, PKC-, EGF receptor (EGFR) tyrosine kinase-, and Src-dependent pathways. Our results also demonstrate that AVP acts as a potent growth factor for IEC-18 cells, inducing DNA synthesis and cell proliferation in the absence of any other exogenously added growth factor through $[Ca^{2+}]_i$-, ERK-, PKC-, EGFR- and Src-dependent pathways. Thus AVP may play an unrecognized role in the maintenance of the small intestinal mucosa by contributing to the regulation of intestinal epithelial cell proliferation and migration.

MATERIALS AND METHODS

Cell culture. IEC-18 cells were purchased from American Type Culture Collection. Stock cultures of these cells were maintained in Dulbecco's modified Eagle's medium (DMEM) supplemented with 5% fetal bovine serum (FBS) in a humidified atmosphere containing 10% CO_2 and 90% air at 37°C. For experimental purposes, cells were plated in 100-mm dishes at 3×10^5 cells/dish in DMEM containing 5% FBS and were allowed to grow to confluence (5–7 days) and then changed to serum-free DMEM for 18–24 h before the experiment.

Assay of DNA synthesis. Confluent, quiescent cultures of IEC-18 cells were washed twice with DMEM and incubated with DMEM-Waymouth's medium (1:1, vol/vol) and various additions as described in Figs. 7–9. After 15 h of incubation at 37°C, ^{3}H-labeled thymidine (0.2 μCi/ml, 1 μM) was added and the cultures were incubated for a further 4 h at 37°C. Cultures were then washed twice with phosphate-buffered saline (PBS) and incubated in 5% trichloroacetic acid at 4°C for 20 min to remove acid-soluble radioactivity, washed with ethanol, and solubilized in 1 ml of 2% Na_2CO_3-0.1 M NaOH. The acid-insoluble radioactivity was determined by scintillation counting in 6 ml of Beckman Readysafe.

Measurement of cell number. For experimental purposes, 5×10^4 IEC-18 cells were subcultured in 35-mm Nunc petri dishes with 2 ml of DMEM containing 1% FBS. At *day 0* (24 h after plating), cultures were washed twice with DMEM to remove residual serum and replaced with DMEM-Waymouth's medium (1:1, vol/vol) with or without vasopressin as described in Fig. 7. Cell number was determined by removing the cells from the dish with a trypsin-EDTA solution (0.5% trypsin in Ca^{2+}- and Mg^{2+}-free PBS with EDTA) and counting a portion of the resulting cell suspension in a Coulter counter. Cell counts were obtained at *day 0* (24 h after plating), *day 1* (48 h after plating), and *day 2* (72 h after plating).

Kinase assay of PKD. Cultures of IEC-18 cells, treated as described in the individual experiments, were washed and lysed in 50 mM Tris·HCl pH 7.6, 2 mM EGTA, 2 mM EDTA, 1 mM dithiothreitol (DTT), 10 μg/ml aprotinin, 10 μg/ml leupeptin, 1 mM 4-(2-aminoethyl)-benzenesulfonyl fluoride HCl (AEBSF), and 1% Triton X-100 (lysis *buffer A*). Cell lysates were clarified by centrifugation at 15,000 *g* for 10 min at 4°C. PKD was immunoprecipitated at 4°C for 2–4 h with the PA-1 antiserum (1:100) as previously described (85). The immune complexes were recovered using protein A coupled to agarose.

PKD autophosphorylation was determined in an in vitro kinase assay by mixing 20 μl of PKD immunocomplexes with 10 μl of a phosphorylation mixture containing (final concentration) 100 μM [γ-^{32}P]ATP (specific activity 400–600 cpm/pmol), 30 mM Tris·HCl pH 7.4, 10 mM $MgCl_2$, and 1 mM DTT. After 10 min of incubation at 30°C the reaction was stopped by washing with 200 μl of kinase buffer and adding an equal volume of 2× SDS-PAGE sample buffer (200 mM Tris·HCl pH 6.8, 2 mM EDTA, 0.1 M Na_3VO_4, 6% SDS, 10% glycerol, and 4% 2-mercaptoethanol), and SDS-PAGE analysis was performed (81, 85). The gels were dried, and the 110-kDa radioactive band corresponding to autophosphorylated PKD was visualized by autoradiography. Autoradiographs were scanned in a GS-710 calibrated imaging densitometer (Bio-Rad), and the labeled band was quantified with Quantity One software program (Bio-Rad).

Western blot analysis for pS916 and ERK-2/ERK-1 activation. Quiescent cultures of IEC-18 cells grown on 100-mm dishes were washed twice with DMEM and then treated as described in the individual experiments. The cells were lysed in 2× SDS-PAGE sample buffer. After SDS-PAGE, proteins were transferred to Immobilon-P membranes (Millipore) and blocked by 3- to 6-h incubation with 5% nonfat milk in PBS, pH 7.2. Membranes were then incubated overnight with the respective primary antibody. PKD activation was determined by incubating the membrane with an antiserum that specifically recognizes the phosphorylated state of serine-916 of PKD (pS916) at a dilution of 1:500 in PBS containing 5% nonfat dried milk.

Activation of ERK-1 and ERK-2 occurs through phosphorylation of specific threonine and tyrosine residues (73), resulting in slower-migrating forms in SDS-PAGE gels. These activated forms were monitored by using a specific anti-phospho-ERK-1/ERK-2 monoclonal antibody (MAb) (New England Biolabs, Beverly, MA) that recognizes the phosphorylated state of Thr^{202} and Tyr^{204} of ERK-1/2. The same membranes were stripped and probed in a similar fashion with goat anti-ERK2 polyclonal antibody.

Bound primary antibodies to immunoreactive bands were visualized by enhanced chemiluminescence detection with horseradish peroxidase-conjugated anti-mouse, anti-rabbit, or anti-goat antibodies. Autoradiograms were scanned using a GS-710 scanner, and the labeled bands were quantified

with Quantity One software. All Western blots shown are representative of at least three independent experiments.

Assay for Pyk2 tyrosine phosphorylation. Confluent cultures of IEC-18 cells were washed with serum-free DMEM, equilibrated in the same medium at 37°C for 3 h, and then treated with AVP. Stimulation was terminated by aspirating the medium and lysing the cells in 1 ml of ice-cold buffer containing 10 mM Tris, pH 7.6, 1% Triton X-100, 50 mM NaCl, 5 mM EDTA, 0.1 mM sodium orthovanadate, 30 mM disodium pyrophosphate, 50 mM NaF, and 1 mM AEBSF. Lysates were clarified by centrifugation at 15,000 rpm for 10 min at 4°C, and the pellets were discarded. Proteins were immunoprecipitated overnight at 4°C with either anti-mouse IgG-agarose linked to monoclonal anti-Tyr(P) [PY-20] or protein A-agarose linked to polyclonal anti-Pyk2 antibody. Immunoprecipitates were washed three times with lysis buffer, extracted for 20 min at 95°C in 2× SDS-PAGE sample buffer (200 mM Tris·HCl pH 6.8, 2 mM EDTA, 6% SDS, 4% 2-mercaptoethanol, and 10% glycerol), and then resolved by SDS-PAGE.

To measure pY402 phosphorylation, confluent serum-starved cultures of IEC-18 cells were immunoprecipitated with polyclonal anti-Pyk2 antibody, followed by Western blot analysis with phosphospecific antibody to Tyr^{402} of Pyk2. To assure equal loading, blots were stripped and reprobed with anti-Pyk2 antibody.

Measurement of $[Ca^{2+}]_i$. $[Ca^{2+}]_i$ was measured with the fluorescent indicator fura 2. Confluent and quiescent cultures of IEC-18 cells, grown on 9 × 22-mm coverslips, were washed twice with Hanks' buffered salt solution (pH 7.2) supplemented with (in mM) 35 $NaHCO_3$, 1.3 $CaCl_2$, 0.5 $MgCl_2$, 0.4 $MgSO_4$, and 0.1% bovine serum albumin (*buffer B*). After washing, cells were incubated with 5 μM fura 2-tetraacetoxymethyl ester (fura 2-AM) for 30 min at room temperature. The cultures were then washed twice with *buffer B*. Each coverslip was placed in a quartz cuvette containing 2 ml of *buffer B*, and fluorescence was measured continuously in a Hitachi F-2000 fluorospectrophotometer, with dual excitation wavelengths of 340 (λ1) and 380 (λ2) nm and an emission wavelength of 510 nm, while the incubation media were continually stirred at 37°C. $[Ca^{2+}]_i$ was determined with the formula

$$[Ca^{2+}]_i(nM) = K_d \frac{(R - R_{min})}{(R_{max} - R)} \times \frac{F_{min}\lambda 2}{F_{max}\lambda 2}$$

where R is the ratio of the emission at 510 nm after excitation at 340 and 380 nm, R_{min} and R_{max} are minimum and maximum R, F_{max} is the fluorescence after the addition of 40 μM digitonin, and F_{min} is the fluorescence after the Ca^{2+} in the solution has been chelated with 10–20 mM EGTA. The value of the dissociation constant (K_d) for Ca^{2+} was 224 nM (29).

Measurement of $[Ca^{2+}]_i$ in individual cells. IEC-18 cells were grown, loaded with fura 2-AM, and washed as described in *Measurement of $[Ca^{2+}]_i$*. The coverslips were then placed in a coverslip chamber with 1 ml of *buffer B*. The chamber was mounted on the stage of a Zeiss 100TV inverted microscope, with a 40× objective (Fluar; Zeiss, New York, NY). Mounted cells were perfused with *buffer B* (~1 ml/min) by using a two-channel peristaltic pump (Rainin, Woburn, MA) at 37°C. $[Ca^{2+}]_i$ was measured with a fluorescent videomicroscopy system (RatioVision, Atto Instruments, Rockville, MD) using 334- and 380-nm excitation filters as described previously (29). Calibration of the fura 2 fluorescence ratios was accomplished in vitro with a series of buffered Ca^{2+} standards containing Mg^{2+}. Perfusion was discontinued before addition of agonists. In general, full ratio images were obtained at sampling rates of 1.0–1.5 images/s.

Wounding assay. IEC-18 cells were plated on 22-mm glass coverslips at 2×10^5 cells/coverslip in DMEM containing 5% FBS. The cell cultures were allowed to grow to confluence (3–5 days) and then changed to serum-free DMEM for 24 h before the experiment. Wounding was initiated by creating linear scrapes through the cell monolayers with a sterile needle as previously described (76). After wounding, the coverslips were washed three times with DMEM and then placed in serum-free medium in the presence or absence of agonists.

To quantitate the rate of cell migration, phase-contrast images were collected with a 10× 0.5-numerical aperture objective. Initial wound quantitation was performed on images collected 20 min after wounding. The wound width was consistently between 520 and 570 μm (mean width 545.3 ± 21.4 μm; $n = 20$). Further images were randomly collected from 10 different wounded areas at 24 h after wounding. Wound-induced migration was calculated as the number of the cells across the initial wound. Data are presented as means ± SE after subtraction of the basal number of migrating cells into the wound seen in the respective controls. Each data point presented in this study represents analysis of images collected from >10 different wounded areas. Differences between groups were analyzed with the unpaired Student's *t*-test. The significance level was defined as $P < 0.05$.

Materials. [γ-^{32}P]ATP (370 MBq/ml) and [^{3}H]thymidine were from Amersham Pharmacia Biotech (Piscataway, NJ). Bisindolylmaleimide I (GF-109203X; GF-I), bisindolylmaleimide V (GF-V), Ro-31-8220, PP-2, PP-3, compound 56, 1,2-bis(2-aminophenoxy)ethane-*N,N,N′,N′*-tetraacetic acid (BAPTA), and genistein were purchased from Calbiochem. AVP, phorbol 12,13-dibutyrate (PDB), EGF, PD-98059, U-0126, V_1 antagonist [β-mercapto-β,β-cyclopentamethylenepriopionyl^1,*O*-Me-Tyr^2,Arg^8]vasopressin, tyrphostin AG-1478, PDB, ionomycin, and trypsin-EDTA solution (1×) were obtained from Sigma (St. Louis, MO). Protein A-agarose was from Boehringer Mannheim. PA-1 antiserum was raised against the synthetic peptide EEREMKALSERVSIL, which corresponds to the carboxy-terminal region of the predicted amino acid sequence of PKD, as previously described (81, 85). Anti-phospho-ERK-1/2 MAb was obtained from New England Biolabs. Anti-ERK2 polyclonal antibody was from Santa Cruz Biotechnology (Santa Cruz, California). An antiserum that specifically recognizes the phosphorylated state of Ser^{916} of PKD (pS916) was generously provided by Dr. Doreen Cantrell (Imperial Cancer Research Fund, London, UK). Other items were from standard suppliers or as specifically indicated.

RESULTS

AVP induces a rapid and transient increase in $[Ca^{2+}]_i$ in IEC-18 cells. The mobilization of Ca^{2+} from intracellular stores leading to a rapid and transient increase in $[Ca^{2+}]_i$ is one of the earliest events stimulated by the binding of agonists to GPCRs that signal through G_q-mediated activation of PLC (5, 20, 66). To identify the expression of G_q-coupled GPCRs in intestinal epithelial cells, multiple peptide hormones were screened for their ability to induce Ca^{2+} mobilization in IEC-18 cells, a nontransformed intestinal epithelial cell line derived from rat ileum (56, 57). These cells were plated onto coverslips and loaded with the fluorescent Ca^{2+} indicator fura 2-AM, and $[Ca^{2+}]_i$ was

continuously recorded as described in MATERIALS AND METHODS. In the course of these studies, we found that AVP induced a marked increase in $[Ca^{2+}]_i$ in IEC-18 cells. As shown in Fig. 1*A*, addition of 50 nM AVP to IEC-18 cells induced a rapid increase in $[Ca^{2+}]_i$ that reached peak values of ~1,000 nM (992 ± 38; $n = 6$) at 20 s and subsequently declined toward a plateau phase.

To determine the extent to which the population $[Ca^{2+}]_i$ response of IEC-18 cells (i.e., the averaged response of thousands of cells, as measured in the fluorimeter cuvette) reflects the behavior of individual cells, we used digital fluorescence image analysis to measure $[Ca^{2+}]_i$ in single cells. As in the analysis of the population of IEC-18 cells, individual cells exhibited a rapid and transient increase in $[Ca^{2+}]_i$ in response to AVP. This Ca^{2+} flux exhibited typical peak and plateau phases, although with small differences in the lag time and magnitude of $[Ca^{2+}]_i$ increase between individual cells (results not shown). Of 50 IEC-18 cells analyzed, 98% responded to AVP, indicating that virtually all cells in the population express receptors for this agonist.

There are at least three GPCR subtypes that bind AVP, namely, V_{1A}, V_{1B}, and V_2 receptors (6). V_{1A} and V_{1B} receptors are known to couple to G_q and thereby to PLC-mediated generation of $Ins(1,4,5)P_3$, which mobilizes Ca^{2+} from internal stores, whereas V_2 receptors activate G_s and stimulate cAMP synthesis. To distinguish the receptor subtype expressed by IEC-18 cells, we used the selective V_{1A} receptor antagonist [β-mercapto-β,β-cyclopentamethyleneproprionyl^1,*O*-Me-Tyr^2,

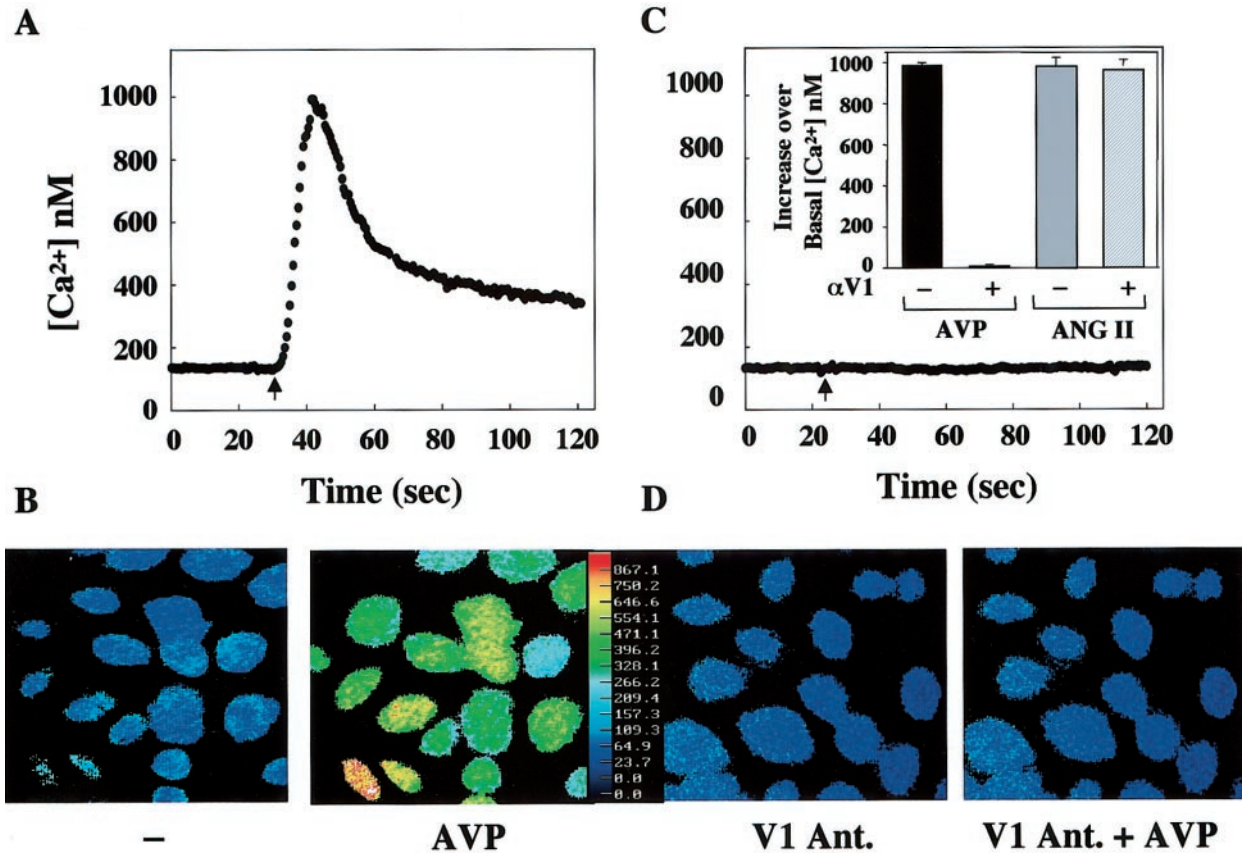

Fig. 1. Arginine vasopressin (AVP) induces a rapid increase in intracellular Ca^{2+} concentration ($[Ca^{2+}]_i$) in IEC-18 cells. *A*: AVP induces a rapid increase in $[Ca^{2+}]_i$ in cell populations. Confluent IEC-18 cells grown on coverslips were washed twice with *buffer B*. $[Ca^{2+}]_i$ after addition of 100 nM AVP was determined as described in MATERIALS AND METHODS. The tracing shown is representative of 6 independent experiments. *B*: AVP increases $[Ca^{2+}]_i$ in single IEC-18 cells. *Left*, cells grown on a coverslip, loaded with 5 μM fura 2-tetraacetoxymethyl ether (AM), and viewed under ×40 objective. Color was added with Adobe Photoshop to reflect $[Ca^{2+}]_i$ in nM. *Right*, the same field of view after addition of 50 nM AVP. *C*: AVP-induced $[Ca^{2+}]_i$ response is prevented by exposure to the selective V_{1A} receptor antagonist [β-mercapto-β,β-cyclopentamethyleneproprionyl^1,*O*-Me-Tyr^2,Arg^8]vasopressin (αV_1). Confluent IEC-18 cells were washed twice with *buffer B* and then incubated without or with 50 nM αV_1 for 30 min. $[Ca^{2+}]_i$ after addition of 100 nM AVP was determined. The tracing shown is representative of 6 independent experiments. *Inset*, the increase in $[Ca^{2+}]_i$ induced by AVP is inhibited by exposure to a selective V_{1A} receptor antagonist. Confluent IEC-18 cells grown on coverslips were washed twice with *buffer B* and then incubated without or with 50 nM αV_1 for 30 min, and $[Ca^{2+}]_i$ after addition of 100 nM AVP or 100 nM ANG II was determined. The bar graph shows mean ± SE increase over basal $[Ca^{2+}]_i$ ($n = 6$). *D*: increase in $[Ca^{2+}]_i$ induced by AVP is prevented by a selective V_{1A} receptor antagonist in the entire IEC-18 cell population. *Left*, confluent IEC-18 cells grown on coverslips were washed twice with *buffer B* and then incubated with 50 nM αV_1 for 30 min. *Right*, the same field of view after addition of 50 nM AVP.

Arg^8]vasopressin (40). Pretreatment of IEC-18 cells plated on coverslips with this selective V_{1A} receptor antagonist completely abolished the transient increase in $[Ca^{2+}]_i$ induced by AVP in IEC-18 cells (Fig. 1, *C* and *D*). In contrast, pretreatment with V_{1A} receptor antagonist had no effect on angiotensin-induced Ca^{2+} mobilization, confirming the selectivity of this antagonist (Fig. 1*C*, *inset*).

AVP induces PKD activation in IEC-18 cells. In addition to Ins(1,4,5)P_3, which induces the rapid release of Ca^{2+} from internal stores, the V_{1A} receptor subtype triggers the PLC-mediated generation of DAG that activates PKC. Downstream targets for PKCs in intestinal epithelial cells have not been clearly defined. PKD is a novel serine/threonine protein kinase that can be distinguished from PKC isoforms by a variety of criteria including catalytic domain structure, substrate specificity, the presence of a pleckstrin homology (PH) domain, and the absence of a pseudosubstrate autoinhibitory motif, which is present in all known PKCs upstream of the first cysteine-rich domain (65). The recent identification of additional distinct cDNA clones, similar in overall structure, primary sequence, and enzymological properties to PKD/PKCμ underscores that PKD isozymes represent a distinct serine protein kinase family, separated from PKCs by many features (34, 75). We recently showed (10) that angiotensin and lysophosphatidic acid (LPA) induce PKD activation in both IEC-6 and IEC-18 cells through a PKC-dependent signal transduction pathway.

To determine whether AVP induces PKD activation in intact IEC-18 cells, cultures of these cells treated with increasing concentrations of AVP were lysed and PKD was immunoprecipitated with PA-1 antiserum. The resulting immunocomplexes were incubated with [γ-^{32}P]ATP, and the incorporation of ^{32}P into PKD was analyzed by SDS-PAGE and autoradiography. As shown in Fig. 2*A*, *top*, stimulation of IEC-18 cells with AVP induced a rapid and striking increase in PKD kinase activity that was maintained during cell lysis and immunoprecipitation. Half-maximal and maximal PKD activation were achieved at 1 and 10 nM, respectively (Fig. 2*A*).

Recently, an antiserum specifically recognizing the phosphorylated form of a PKD carboxy-terminal residue, Ser^{916}, was developed and used to detect in vivo autophosphorylation at this site by active PKD (47). Thus the pS916 antiserum provides a novel approach for detecting conversion of PKD to an active form within cells. Here, lysates from IEC-18 cells stimulated with increasing concentrations of AVP were analyzed by SDS-PAGE followed by Western blot analysis with the pS916 antiserum. AVP stimulation induced a dramatic increase in the immunoreactivity of the PKD band indicative of phosphorylation at Ser^{916} (Fig. 2A, *middle*).

Stimulation of intact IEC-18 cells with AVP for various times induced a striking time-dependent increase in PKD activation, as judged by assays of in vitro PKD kinase activity after immunoprecipitation or by Western blotting with pS916 antibody to detect PKD autophosphorylation in intact cells (Fig. 2*B*). PKD activation was detectable within 30 s and reached a maximum (~10-fold) after 1 min of AVP stimulation. These results demonstrate that PKD activation is one of the early events induced by AVP in IEC-18 cells.

We also examined the effect of AVP on PKD activation monitored by PKD autophosphorylation at Ser^{916} at longer times. As shown in Fig. 2*C*, AVP-induced PKD activation within cells declined gradually toward baseline levels. In contrast, PKD activation induced by PDB persisted for at least 90 min of treatment. Thus AVP-induced PKD activation is transient compared with that induced by PDB.

As shown with AVP-induced calcium mobilization, AVP-induced PKD activation was also prevented by pretreatment of these cells with the selective V_{1A} receptor antagonist [β-mercapto-β,β-cyclopentamethyleneproprionyl^1,*O*-Me-Tyr^2,Arg^8]vasopressin (Fig. 2*D*). In contrast, pretreatment with this V_{1A} receptor antagonist had no effect on PKD activation in response to either angiotensin II or PDB (Fig. 2*D*).

AVP stimulates PKD activation via PKC. To determine the role of PKCs in PKD activation induced by AVP, cultures of IEC-18 cells were treated with various concentrations of the selective PKC inhibitors GF-I (78) and Ro-31-8220 (84) before AVP stimulation. As shown in Fig. 3*A*, *top*, treatment with GF-I potently blocked PKD activation induced by subsequent addition of AVP in a concentration-dependent fashion. In contrast, GF-I added directly to the in vitro kinase assay, even at the concentrations (0.25–2.5 μM) that abrogated AVP-induced PKD activation in intact IEC-18 cells, did not inhibit PKD activity (Fig. 3*A*, *middle*). Similar results were obtained when the PKC inhibitor Ro-31-8220 was used instead of GF-I (Fig. 3*B*). These results imply that Ro-31-8220 and GF-I do not inhibit PKD activity directly but interfere with AVP-mediated PKD activation in intact cells by blocking PKC. In addition to in vitro kinase assays (Fig. 3, *A* and *B*), pretreatment of IEC-18 cells with PKC inhibitors also blocked AVP-induced PKD autophosphorylation at Ser^{916} in intact cells (Fig. 3*C*).

In contrast to the results obtained with GF-I and Ro-81-3220, treatment of IEC-18 cells with the broad-spectrum protein tyrosine kinase inhibitor genistein, the phosphoinositide 3-kinase inhibitor wortmannin (52), the selective EGFR tyrosine kinase inhibitor tyrphostin AG-1478 (43), or the selective Src family kinase inhibitor PP-2 (33) did not interfere with AVP-induced PKD activation (Fig. 3*D*). These results demonstrate the specificity of the PKC inhibitors and indicate that these kinases are not upstream regulators of PKD.

AVP induces Pyk2 tyrosine phosphorylation and Src activation. An elevation in $[Ca^{2+}]_i$ and an increase in PKC activity stimulate activation and tyrosine phosphorylation of the cytosolic proline-rich tyrosine kinase 2 (Pyk2) in a variety of cell types (41, 42, 72). Because initial results indicated that Pyk2 is expressed by IEC-18 cells, we examined whether AVP can stimulate Pyk2 tyrosine phosphorylation in these cells. Confluent

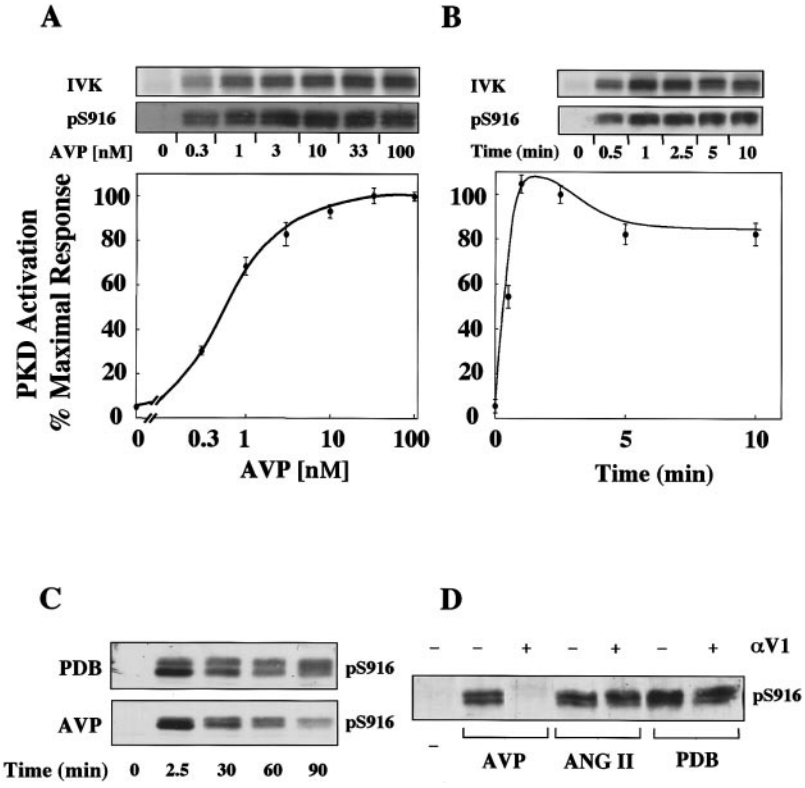

Fig. 2. AVP activates protein kinase D (PKD) in a time- and dose-dependent manner through the V_{1A} receptor. *A*: AVP dose-response curve. *Top*, confluent and quiescent cultures of IEC-18 cells were treated with various concentrations of AVP for 2.5 min at 37°C as indicated. The cultures were lysed in lysis *buffer A* and immunoprecipitated with PA-1 antiserum, and PKD activity was determined by an in vitro kinase assay (IVK) as described in MATERIALS AND METHODS. The autoradiogram shown is representative of at least 3 independent experiments. *Middle*, identical experiments were carried out in parallel cultures where Western blot analysis with pS916 antiserum was performed after lysis of the cells with 2× sample buffer as described in MATERIALS AND METHODS. The blot shown is representative of at least 3 independent experiments. *Bottom*, results are means ± SE (n = 3) of the level of PKD activation from IVK obtained from scanning densitometry expressed as % of the maximum increase in phosphorylation obtained with 100 nM AVP. *B*: *top*, AVP time course. Confluent and quiescent cultures of IEC-18 cells were treated for various times with 100 nM AVP at 37°C as indicated. Cells were lysed and immunoprecipitated with PA-1 antiserum to isolate PKD for IVK. The autoradiogram shown is representative of at least 3 independent experiments. *Middle*, identical experiments were carried out in parallel cultures where Western blot analysis with pS916 antiserum was performed after lysis of the cells with 2× sample buffer. The blot shown is representative of 3 independent experiments. *Bottom*, results are the means ± SE (n = 3) of the level of PKD activation obtained from scanning densitometry expressed as % of the maximum increase in phosphorylation obtained from cells incubated with 100 nM AVP at 37°C. *C*: confluent serum-starved cultures of IEC-18 cells were treated for various times with 100 nM AVP or 100 nM phorbol 12,13-dibutyrate (PDB) at 37°C as indicated. Western blot analysis with pS916 antiserum was performed after lysis of the cells with 2× sample buffer. *D*: confluent quiescent IEC-18 cultures were incubated for 1 h without or with αV_1 (10 nM). The cultures were subsequently left unstimulated (−) or stimulated (+) for 2.5 min with 10 nM AVP, 100 nM ANG II, or 100 nM PDB. Western blot analysis with pS916 antiserum was performed after lysis of the cells with 2× sample buffer.

cultures of IEC-18 cells were treated with increasing concentrations of AVP and lysed, and extracts were immunoprecipitated with anti-Tyr(P) antibody. The resulting immunocomplexes were analyzed by SDS-PAGE followed by Western blotting with anti-Pyk2 antibody. As shown in Fig. 4*A*, AVP induced a striking increase in the tyrosine phosphorylation of Pyk2, indicative of activation. Half-maximal and maximal activation were achieved at 3 and 10 nM, respectively. Stimulation of IEC-18 cells with AVP for various times indicated that AVP induced rapid Pyk2 tyrosine phosphorylation, reaching a maximum within 1 min (Fig. 4*B*). Similar results were obtained when the tyrosine phosphorylation of Pyk2 was assessed by immunoprecipitation with an anti-Pyk2 antibody followed by Western blotting with an anti-phosphotyrosine antibody (results not shown).

The major autophosphorylation site of Pyk2 is Tyr^{402} (2). To determine whether AVP induces Pyk2 phosphorylation at Tyr^{402}, serum-starved cultures of IEC-18 cells were incubated with or without AVP and immunoprecipitated with anti-Pyk2 antibody, followed by Western blotting with a phosphospecific antibody to Tyr^{402}. As shown in Fig. 4*C*, *left*, AVP stimulation induced phosphorylation of Pyk2 at Tyr^{402}. We verified that similar amounts of Pyk2 were immunoprecipitated from lysates of IEC-18 cells treated with or without AVP (Fig. 4*C*, *right*).

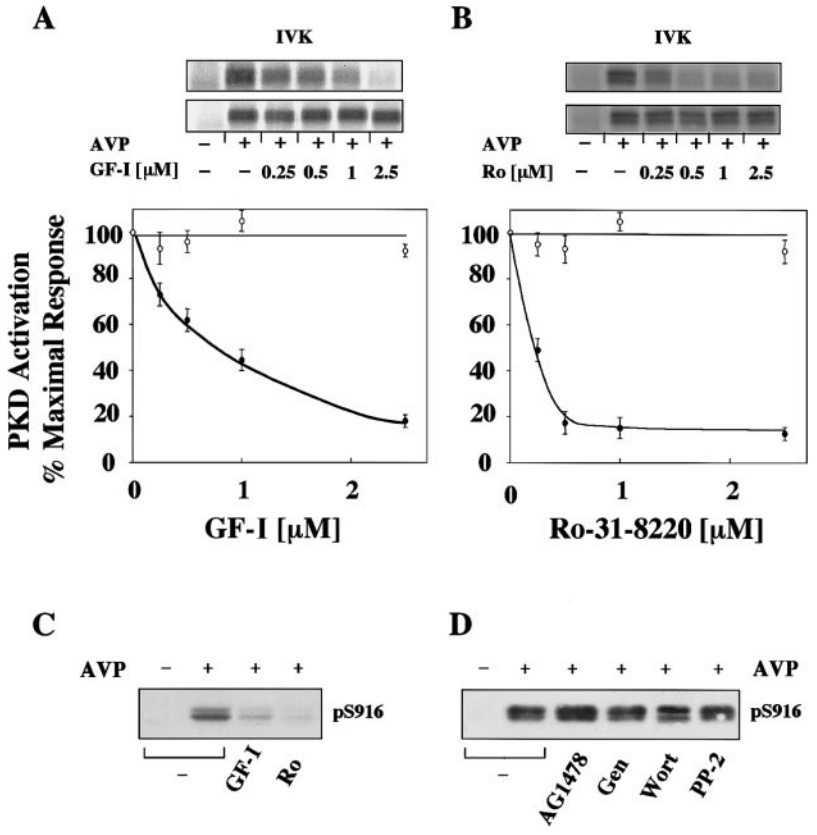

Fig. 3. AVP stimulates PKD activation through a PKC-dependent pathway. *A*: treatment of intact cells with GF-109203X (GF-I) inhibits PKD activation. Confluent IEC-18 cells were incubated for 1 h with different concentrations of the PKC inhibitor GF-I (*top* and *C*). Control cells (−) received equivalent amount of solvent. The cultures were subsequently stimulated for 2.5 min with 100 nM AVP at 37°C. Cells were lysed with lysis *buffer A* and immunoprecipitated with PA-1 antiserum. PKD activity was then determined by IVK. Parallel cultures were treated with 100 nM AVP for 2.5 min at 37°C (*middle*). Cells were lysed with lysis *buffer A* and immunoprecipitated with PA-1 antiserum. PKD activity was then determined by IVK in absence or presence of the indicated concentrations of GF-I added to the incubation mixture. *Bottom,* results are means ± SE (n = 3) of the level of PKD activation obtained from scanning densitometry expressed as % of the maximum increase in phosphorylation obtained from cells incubated with 100 nM AVP for 90 s at 37°C. ●, Values corresponding to PKD activity from cells incubated with GF-I; ○, values corresponding to PKD activity determined by IVK in the absence or presence of the indicated concentrations of GF-I added to the incubation mixture. B: Ro-31-8220 inhibits PKD activity. Confluent IEC-18 cells were incubated for 1 h with different concentrations of the PKC inhibitor Ro-31-8220 (*top* and *D*). Control cells (−) received equivalent amount of solvent. The cultures were subsequently stimulated for 2.5 min with 100 nM AVP at 37°C. Cells were lysed and immunoprecipitated with PA-1 antiserum to isolate PKD for IVK. Parallel cultures were treated with 100 nM AVP for 2.5 min at 37°C (*middle*). Cells were lysed with lysis *buffer A* and immunoprecipitated with PA-1 antiserum. PKD activity was then determined by IVK in the absence or presence of the indicated concentrations of Ro-31-8220 added to the incubation mixture. *Bottom,* results are means ± SE (n = 3) of the level of PKD activation obtained from scanning densitometry expressed as % of the maximum increase in phosphorylation obtained from cells incubated with 100 nM AVP for 90 s at 37°C. ●, Values corresponding to PKD activity from cells incubated with Ro-31-8220; ○, values corresponding to PKD activity determined by IVK in the absence or presence of the indicated concentrations of Ro-31-8220 added to the incubation mixture. *C*: confluent serum-starved IEC-18 cells were incubated for 1 h with 3.5 μM GF-I, 2.5 μM Ro-31-8220, or equivalent amount of solvent. The cultures were subsequently left unstimulated (−) or stimulated (+) for 2.5 min with 10 nM AVP at 37°C. Western blot analysis with pS916 antiserum was performed after lysis of the cells with 2× sample buffer. *D*: confluent serum-starved IEC-18 cells were incubated for 30 min with 10 μM PP-2 and for 1 h with 250 nM tyrphostin AG-1478, 50 μM genistein (Gen), 100 nM wortmannin (Wort), or equivalent amount of solvent. The cultures were subsequently left unstimulated (−) or stimulated (+) for 2.5 min with 10 nM AVP at 37°C. Western blot analysis with pS916 antiserum was performed after lysis of the cells with 2× sample buffer. All Western blots shown are representative of 3 independent experiments.

The phosphorylation of Pyk2 at Tyr^{402} creates a potential high-affinity binding site for the SH2 domain of Src, leading to Src activation (2). The increase in the activity of Src in intact cells can be detected by monitoring its phosphorylation at Tyr^{418}, an autophosphorylation site located in the kinase activation loop. To examine whether AVP stimulates Src activation in IEC-18 cells, confluent cultures of these cells were treated for various times with 10 nM AVP followed by Western blotting with a phosphospecific antibody that recognizes only the activated form phosphorylated on Tyr^{418}. Stimulation of IEC-18 cells with AVP for vari-

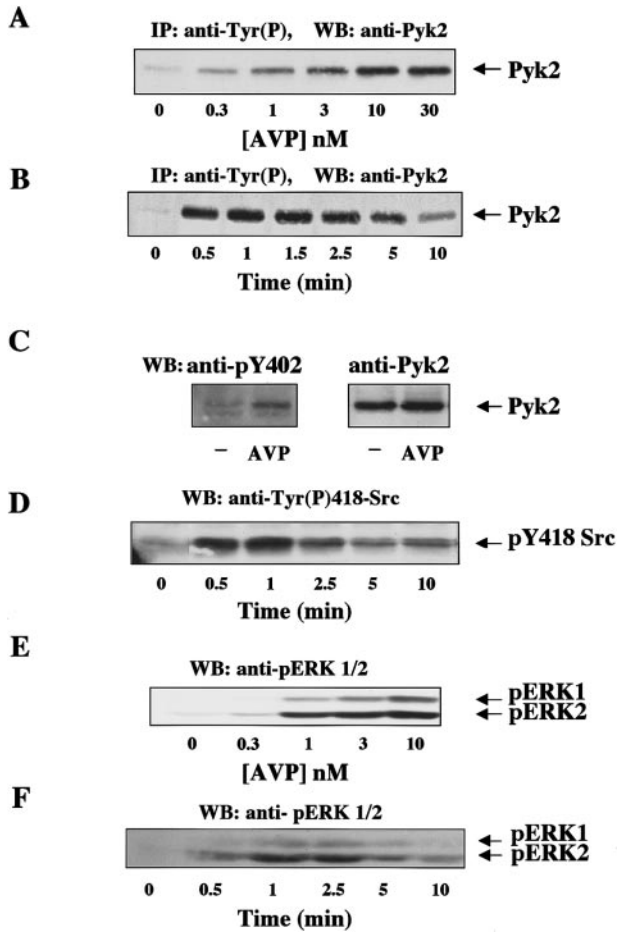

Fig. 4. AVP induces proline-rich tyrosine kinase 2 (Pyk2) tyrosine phosphorylation, Src activation, and extracellular signal-regulated kinase (ERK)-1/2 activation in IEC-18 cells. *A*: dose response of Pyk2 tyrosine phosphorylation induced by AVP. Confluent IEC-18 cells were washed and incubated at 37°C for 1 min with various concentrations of AVP as indicated. Cells were then lysed, and extracts were immunoprecipitated (IP) with anti-Tyr(P) antibody (PY20) followed by Western blotting (WB) with anti-Pyk2 antibody. *B*: time course of Pyk2 tyrosine phosphorylation induced by AVP. Confluent IEC-18 cells were washed and incubated at 37°C with 100 nM AVP for various times as indicated, and cell lysates were analyzed for Pyk2 phosphorylation as described in *A*. C: AVP stimulates Pyk2 autophosphorylation at Tyr^{402}. Confluent IEC-18 cells were washed and incubated at 37°C for 1 min with 100 nM AVP. *Left*, cells were then lysed and immunoprecipitated with anti-Pyk2 antibody followed by Western blotting with phosphospecific antibody for Tyr^{402}. *Right*, the same blot was stripped and reprobed for total Pyk2, indicating equal loading. *D*: AVP induces rapid Src autophosphorylation in IEC-18 cells. Confluent quiescent cultures of IEC-18 cells were treated for various times with 100 nM AVP at 37°C as indicated. Western blot analysis with a phosphospecific antibody that recognizes the activated form phosphorylated on Tyr^{418} was performed after lysis of the cells with 2× sample buffer. *E*: AVP induces $p42^{mapk}$ (ERK-2) and $p44^{mapk}$ (ERK-1) phosphorylation in a dose-dependent manner. Confluent quiescent cultures of IEC-18 cells were treated with various concentrations of AVP for 2.5 min at 37°C as indicated. Western blot analysis with a specific anti-phospho-ERK-1/2 monoclonal antibody (MAb) that recognizes only the activated forms phosphorylated on Thr^{202} and Tyr^{204} was performed after lysis of the cells with 2× sample buffer. *F*: AVP induces $p42^{mapk}$ (ERK-2) and $p44^{mapk}$ (ERK-1) phosphorylation in a time-dependent manner. Confluent quiescent cultures of IEC-18 cells were treated for various times with 10 nM AVP at 37°C as indicated, and Western blot analysis with a specific anti-phospho-ERK-1/-2 MAb was performed.

ous times shows that this hormone induces Src activation rapidly in these cells, reaching a maximum within 1 min (Fig. 4*D*). Thus the kinetics of Src activation parallels that of Pyk2 tyrosine phosphorylation.

AVP stimulates ERK-1/2 activation via V_{1A} receptor and is dependent on ERK kinase. The MAPKs are a family of highly conserved serine/threonine kinases that are activated by a range of extracellular signals via protein phosphorylation cascades that relay mitogenic signals to the nucleus (83). The two best characterized isoforms, ERK-1 ($p44^{mapk}$) and ERK-2 ($p42^{mapk}$), are directly activated by phosphorylation on specific tyrosine and threonine residues by the dual-specificity ERK kinase (or MAPK kinase; MEK) (83). In some cell types, activation of Pyk2 and Src family kinases triggers the stimulation of the Raf-MEK-ERK cascade via Ras activation (30, 66).

To examine whether AVP induces ERK-1/2 activation in IEC-18 cells, cultures of these cells were treated with increasing concentrations of AVP and lysed, and the active forms of ERK-1/2 were detected by Western blotting with an antibody that recognizes the dually phosphorylated forms of these enzymes. As illustrated in Fig. 4*E*, AVP induced ERK activation in a concentration-dependent fashion, achieving half-maximal and maximal activation at 1 and 10 nM, respectively. Addition of AVP at higher concentrations (up to 1 μM) did not give increased ERK phosphorylation beyond that achieved at 10 nM (data not shown). Stimulation of IEC-18 cells with AVP for various times indicates that AVP induces ERK activation rapidly, reaching a maximum within 1 min (Fig. 4*F*).

As other early signals induced by AVP in IEC-18 cells, AVP-induced ERK activation was also prevented by pretreatment of these cells with the selective V_{1A} receptor antagonist [β-mercapto-β,β-cyclopentamethyleneproprionyl^1,*O*-Me-Tyr^2,Arg^8]vasopressin (Fig. 5*A*).

To determine whether AVP-induced activation of ERK-1/2 is mediated by MEK in IEC-18 cells, cultures of these cells were preincubated for 1 h in the absence or presence of the specific MEK inhibitor PD-98059 (3) and subsequently stimulated with AVP. The results shown in Fig. 5*B* demonstrate that exposure to PD-98059 completely prevented ERK activation in response to AVP. Recently, U-0126, a compound structurally unrelated to PD-98059, has been identified as a potent and specific inhibitor of MEK-1 and MEK-2 (21). As shown in Fig. 5*B*, ERK activation in response to AVP was also abrogated by prior exposure to U-0126.

Role of PKC, Src, $[Ca^{2+}]_i$, and EGFR in AVP-stimulated ERK-1/2 activation. To investigate the upstream pathway(s) leading to MEK activation, we examined the contribution of PKC, $[Ca^{2+}]_i$, Src, and EGFR to AVP-induced ERK activation. As shown in Fig. 5*C*, pretreatment of cells with the specific PKC inhibitors GF-I and Ro-31-8220 prevented AVP-induced ERK activation. In contrast, preincubation of cultures with GF-V, a biologically inactive analog of GF-I, had no effect on AVP-induced ERK activation.

To test whether tyrosine kinases may be involved in AVP-induced ERK activation, cultures of cells were

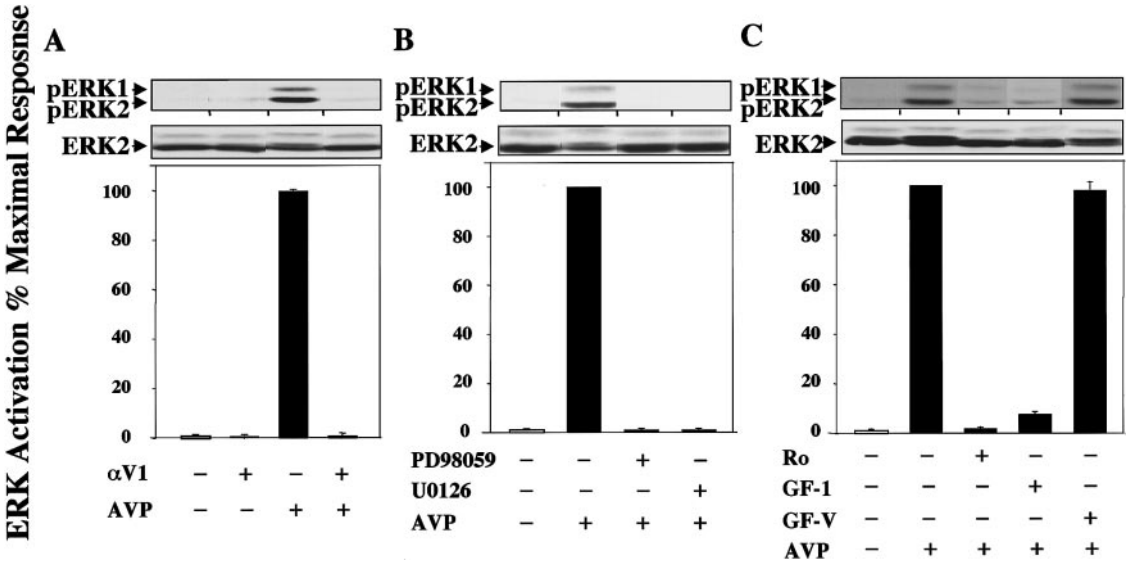

Fig. 5. Effect of V_{1A} antagonist and inhibitors of ERK kinase (or MAPK kinase, MEK) and PKC on AVP-induced ERK-1/2 phosphorylation. *A*: confluent quiescent IEC-18 cultures were incubated for 1 h without or with selective V_{1A} receptor antagonist (αV_1). The cultures were subsequently left unstimulated (−) or stimulated (+) for 2.5 min with 10 nM AVP at 37°C, and Western blot analysis with a specific anti-phospho-ERK-1/2 MAb was performed. Results are means ± SE (n = 3) of the level of ERK-2 and -1 phosphorylation obtained from scanning densitometry expressed as % of the maximum increase in phosphorylation obtained with 10 nM AVP. The Western blot shown is representative of 3 independent experiments. *Middle*, the Western blot was also probed for total ERK, showing equal loading. *B*: MEK inhibitors abolish AVP-induced ERK-2 and ERK-1 phosphorylation. Confluent and quiescent IEC-18 cells were incubated for 1 h with 10 μM PD-98059 or 2.5 μM U-0126. Control cells received equivalent amount of solvent (−). The cultures were subsequently unstimulated (−) or stimulated (+) for 2.5 min with 10 nM AVP at 37°C. Results are means ± SE (n = 3) of the level of ERK-2 and -1 phosphorylation obtained from scanning densitometry expressed % of the maximum increase in phosphorylation obtained with 10 nM AVP. The Western blot shown is representative of 3 independent experiments. *Middle*, the Western blot was also probed for total ERK, showing equal loading. *C*: Ro-31-8220 and GF-I inhibit AVP-induced ERK activation. Confluent quiescent IEC-18 cells were incubated for 1 h with 2.5 μM Ro-31–8220 or 2.5 μM GF-I. Control cells received equivalent amount of solvent (−) or GF-V, a biologically inactive analog of GF-I. The cultures were subsequently unstimulated (−) or stimulated (+) for 2.5 min with 10 nM AVP at 37°C. Results are means ± SE (n = 3) of the level of ERK-2 and -1 phosphorylation obtained from scanning densitometry expressed as % of the maximum increase in phosphorylation obtained with 10 nM AVP. The Western blot shown is representative of 3 independent experiments. *Middle*, the Western blot was also probed for total ERK, showing equal loading.

pretreated with the broad-spectrum tyrosine kinase inhibitor genistein before addition of AVP. Genistein nearly abolished AVP-induced ERK activation (Fig. 6*A*). Our results demonstrating that AVP stimulates Pyk2 and Src activation suggested that genistein could be acting via inhibition of Src family kinases. Indeed, pretreatment of cell cultures with the selective Src kinase inhibitor PP-2 (33) abrogated AVP-induced ERK-1/2 phosphorylation in a concentration-dependent manner (Fig. 6*A*). In contrast, pretreatment with PP-3, a biologically inactive analog of PP-2, had no effect on AVP-induced ERK activation.

To examine the contribution of Ca^{2+} to AVP-induced ERK activation, cultures of cells were pretreated simultaneously for 30 min with thapsigargin to deplete intracellular Ca^{2+} stores and EGTA to chelate extracellular Ca^{2+}. The cell cultures were subsequently left unstimulated or stimulated with AVP either with or without readdition of Ca^{2+}. Depletion of Ca^{2+} by this maneuver (Fig. 6*B*) attenuated AVP-induced ERK-1/2 phosphorylation by ~65%. Readdition of Ca^{2+} to this previously Ca^{2+}-depleted medium completely restored AVP-induced ERK-1/2 phosphorylation in response to AVP, whereas readdition of Ca^{2+} alone to this medium had no stimulatory effect on ERK-1/2 activation.

A variety of GPCR agonists also induce a rapid increase in EGFR tyrosine autophosphorylation in several cell types (12–14, 37, 80), a receptor crosstalk mediated by rapid proteolytic generation of EGFR ligands at the cell surface (55) and termed transactivation (9, 55). To examine whether EGFR transactivation is involved in AVP-induced ERK-1/2 phosphorylation, cultures of cells were pretreated with the selective EGFR tyrosine kinase inhibitor tyrphostin AG-1478 at various concentrations before addition of AVP. AG-1478 (62.5–250 nM) clearly abolished AVP-induced ERK-1/2 activation in a concentration-dependent manner (Fig. 6*C*). Furthermore, pretreatment of cell cultures with another structurally unrelated EGFR tyrosine kinase inhibitor, compound 56 (7, 26, 32), also inhibited AVP-induced ERK-1/2 phosphorylation.

AVP induces DNA synthesis and cell proliferation. Having established that AVP triggers the activation of multiple early pathways that potentially can lead to cell growth, our next step was to determine whether AVP induces cell cycle activation leading to S phase

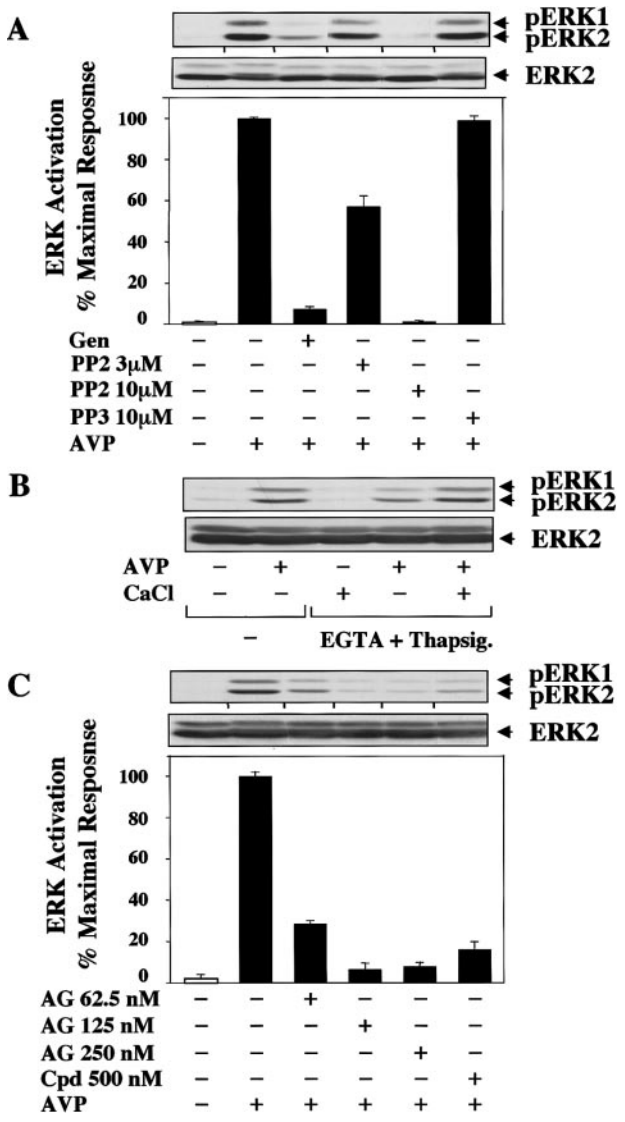

Fig. 6. Effects of Src family kinases and epidermal growth factor receptor (EGFR) tyrosine kinase inhibition on AVP-induced ERK-1/2 phosphorylation. A: genistein and PP-2 abrogate ERK-2 and -1 phosphorylation in response to AVP. *Top*, confluent quiescent IEC-18 cells were incubated for 30 min with 50 μM genistein (Gen), 3 μM PP-2, or 10 μM PP-2. Control cells received equivalent amount of solvent (−) or 10 μM PP-3, a biologically inactive analog of PP-2. The cultures were subsequently unstimulated (−) or stimulated (+) for 2.5 min with 10 nM AVP at 37°C. *Middle*, the Western blot was also probed for total ERK, showing equal loading. *B:* confluent serum-starved IEC-18 cells were treated in the absence (−) or presence (+) of 3 mM EGTA and 50 nM thapsigargin for 30 min. The cell cultures were subsequently left unstimulated (−) or stimulated (+) for 2.5 min with 10 nM AVP with or without 1.8 mM CaCl at 37°C. *Top*, Western blot analysis with a specific anti-phospho-ERK-1/2 MAb was performed. All Western blots shown are representative of at least 3 independent experiments. *Bottom*, the western blot was also probed for total ERK, showing equal loading. *C*: tyrphostin AG-1478 and compound 56 inhibit AVP-induced ERK-1/2 phosphorylation. *Top*, confluent and quiescent IEC-18 cells were incubated for 1 h with various concentrations of EGFR tyrosine kinase inhibitors, AG-1478 (AG), and compound 56 (Cpd). The cultures were subsequently unstimulated (−) or stimulated (+) for 2.5 min with 10 nM AVP at 37°C. *Middle*, the Western blot was also probed for total ERK, showing equal loading. *A* and *C*, *bottom*: results are means ± SE (n = 3) of the level of ERK-2 and ERK-1 phosphorylation obtained from scanning densitometry expressed as % of the maximum increase in phosphorylation obtained with 10 nM AVP. Western blots shown are representative of 3 independent experiments.

entry in IEC-18 cells. Quiescent, serum-deprived cultures of these cells were incubated with increasing concentrations of AVP, and DNA synthesis was assessed by measuring [^{3}H]thymidine incorporation into acid-precipitable material. As shown in Fig. 7*A*, AVP induced a marked increase in [^{3}H]thymidine incorporation in a concentration-dependent fashion, achieving half-maximal and maximal stimulation at ~1 and 10 nM, respectively. A transient exposure of IEC-18 cells to AVP (4 h) was sufficient to induce 50% of the maximum stimulation induced by continuous exposure to AVP (data not shown).

Pretreatment of cells with the selective V_1 receptor antagonist [β-mercapto-β,β-cyclopentamethylenepropionyl^1,*O*-Me-Tyr^2,Arg^8]vasopressin prevented AVP-induced [^{3}H]thymidine incorporation. Interestingly, AVP was more effective than EGF (at 5 ng/ml) in stimulating [^{3}H]thymidine incorporation in IEC-18 cells (Fig. 7*B*). Furthermore, exposure of these cells to both AVP and EGF induced additive stimulation of DNA synthesis that reached a level almost comparable to that promoted by addition of medium containing 5% FBS.

We also determined whether AVP can stimulate IEC-18 cell proliferation in the absence of any other exogenously added growth factor. Sparse cultures of these cells were transferred to serum-free DMEM-Waymouth's medium and then supplemented with or without 100 nM AVP. Cell number was determined by counting trypsinized cells with a Coulter counter. As illustrated in Fig. 7*C*, there is nearly a doubling in the cell number of cultures treated with AVP for 24 and 48 h compared with the controls. The results presented in Fig. 7 indicate that AVP acts as a potent growth factor for IEC-18 cells.

AVP-induced mitogenesis is dependent on MEK, PKC, $[Ca^{2+}]_i$, EGFR tyrosine kinase, and Src family kinase activity. In an effort to elucidate the signal transduction pathways that mediate mitogenic signaling in response to AVP in IEC-18 cells, we examined the effect of treatment with selective inhibitors of the signaling pathways characterized in this study (Figs. 1–6) on the stimulation of DNA synthesis induced by AVP in these cells. To determine whether DNA synthesis in response to AVP is mediated by MEK-dependent ERK-1/2 activation, serum-deprived cultures of IEC-18 cells were preincubated for 1 h in the absence or presence of the specific MEK inhibitors PD-98059 or the structurally unrelated compound U-0126 and subsequently stimulated with AVP. As shown in Fig. 8*A*, treatment with either PD-98059 or U-0126 attenuated [^{3}H]thymidine incorporation in response to AVP stimulation by ~50%.

Because we demonstrated that AVP induces ERK activation through PKC-, Ca^{2+}-, Src- and EGFR-dependent pathways in IEC-18 cells (Figs. 5*C*, 6*A*) and ERK activity is required for AVP-stimulated DNA synthesis (Fig. 8*A*), we hypothesized that the pathways upstream of ERK (i.e., PKC, Ca^{2+}, Src, and EGFR) are also required for reinitiation of DNA synthesis in response to AVP. To test whether AVP-induced DNA

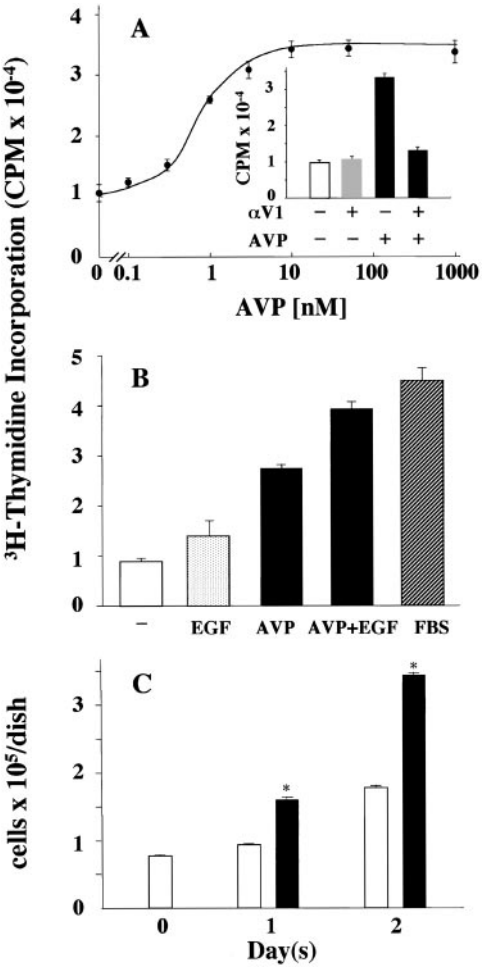

Fig. 7. AVP induces DNA synthesis and cell proliferation in IEC-18 cells. *A*: AVP induces DNA synthesis in IEC-18 cells in a concentration-dependent fashion. Confluent quiescent cultures of IEC-18 cells were washed and incubated at 37°C in 2 ml of DMEM-Waymouth's medium containing increasing concentrations of AVP. After 15 h 1 μCi/ml ^{3}H-labeled thymidine was added to the cultures, and 4 h later DNA synthesis was assessed by measuring the [^{3}H]thymidine incorporated into acid-precipitable material. Results are means ± SE (n = 3). *Inset*, confluent quiescent cultures of IEC-18 cells were washed and incubated at 37°C in 2 ml of DMEM-Waymouth's medium containing 50 nM AVP without or with 50 nM αV_1. After 15 h 1 μCi/ml [^{3}H]thymidine was added to the cultures, and 4 h later DNA synthesis was assessed by measuring the [^{3}H]thymidine incorporated into acid-precipitable material. Results are means ± SE (n = 3). *B*: AVP is a more effective mitogen than EGF. Confluent quiescent cultures of IEC-18 cells were washed and incubated at 37°C in 2 ml of DMEM-Waymouth's medium containing vehicle, 5 ng/ml EGF, 50 nM AVP, 5 ng/ml EGF and 50 nM AVP, or 5% FBS, and [^{3}H]thymidine incorporation was determined. Results are means ± SE (n = 3). *C*: AVP stimulates IEC-18 cell proliferation. Suspended IEC-18 cells (5×10^4) were plated onto 35-mm Nunc petri dishes with 2 ml of DMEM containing 1% FBS. At *day 0* (24 h after plating), cultures were washed twice with DMEM to remove residual serum and replaced with DMEM-Waymouth's medium (1:1, vol/vol) with (open bars) or without (closed bars) 100 nM AVP. Cell number was determined by counting trypsinized cells with a Coulter counter. Cell counts were obtained 24 h after plating (*day 0*) and 24 (*day 1*) and 48 (*day 2*) h after AVP exposure. *$P < 0.01$ vs. DMEM control for respective day.

synthesis is PKC dependent, cells were preincubated for 1 h with the selective PKC inhibitor GF-I (at 3.5 μM) whereas control cells received either an equivalent amount of solvent or GF-V (also at 3.5 μM), a biologically inactive analog of GF-I, before addition of AVP. As shown in Fig. 8*B*, GF-I markedly reduced [^{3}H]thy-

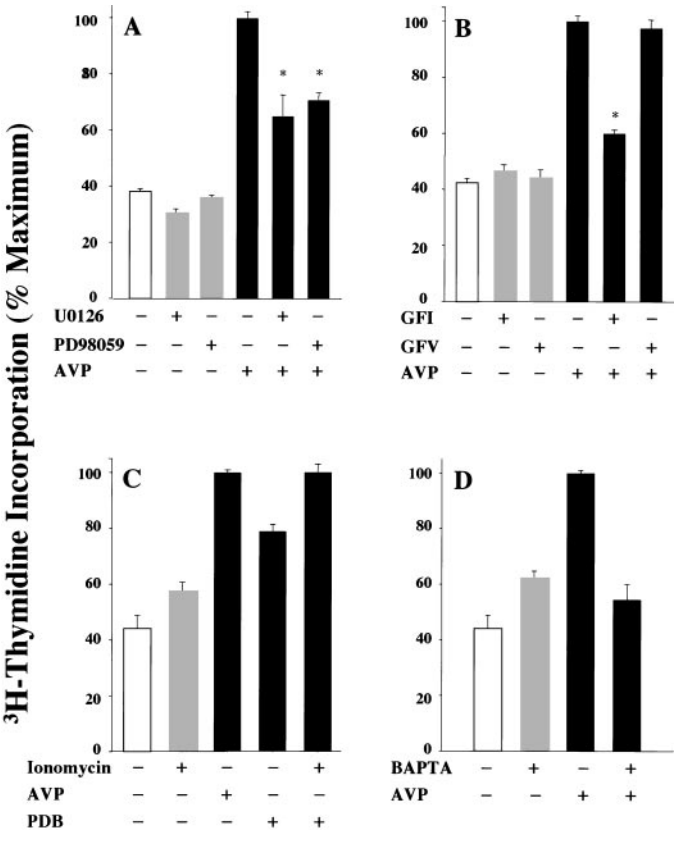

Fig. 8. AVP-induced DNA synthesis is dependent on MEK, PKC, and $[Ca^{2+}]_i$. *A*: effect of the MEK inhibitors PD-98059 or U-0126 on DNA synthesis in response to AVP. Confluent quiescent cultures of IEC-18 cells were washed and incubated at 37°C in 2 ml of DMEM-Waymouth's medium containing 50 nM AVP in the absence or in the presence of 10 μM PD-98059 or 2.5 μM U-0126. After 15 h 1 μCi/ml [^{3}H]thymidine was added to the cultures, and 4 h later DNA synthesis was assessed by measuring the [^{3}H]thymidine incorporated into acid-precipitable material. Results are expressed as mean ± SE % of the maximum increase (n = 3) obtained with 50 nM AVP. *B:* effects of GF-I on DNA synthesis in response to AVP. Confluent quiescent cultures of IEC-18 cells were washed and incubated at 37°C in 2 ml of DMEM-Waymouth's medium containing 50 nM AVP in the absence or presence of GF-I or its inactive analog, GF-V, and [^{3}H]thymidine incorporation into acid-precipitable material was measured. Results are expressed as mean ± SE % of the maximum increase (n = 3) obtained with 50 nM AVP. *C*: effects of ionomycin on DNA synthesis in response to PDB. Confluent quiescent cultures of IEC-18 cells were washed and incubated at 37°C in 2 ml of DMEM-Waymouth's medium containing 100 nM PDB in the absence or in the presence of 10 nM ionomycin, and [^{3}H]thymidine incorporation into acid-precipitable material was measured. Results are expressed as mean ± SE % of the maximum increase (n = 3) obtained with 50 nM AVP. *D*: effects of BAPTA on DNA synthesis in response to AVP. Confluent quiescent cultures of IEC-18 cells were washed and incubated at 37°C in 2 ml of DMEM-Waymouth's medium containing 50 nM AVP in the absence or in the presence of 10 μM BAPTA, and [^{3}H]thymidine incorporation into acid-precipitable material was measured. Results are expressed as mean ± SE % of the maximum increase (n = 3) obtained with 50 nM AVP. *$P < 0.01$ vs. 50 nM AVP.

midine incorporation in response to AVP stimulation by ~70%.

To complement our data with pharmacological agents to inhibit PKC, we also tested whether direct activation of PKC by the phorbol ester PDB can stimulate DNA synthesis. As shown in Fig. 8*C*, addition of PDB to IEC-18 cells incubated in serum-free medium increased [^{3}H]thymidine incorporation by 1.8-fold ($P < 0.05$; $n = 3$).

We used two different approaches to determine the role of $[Ca^{2+}]_i$ in AVP-induced DNA synthesis. As illustrated in Fig. 8*C*, addition of the Ca^{2+} ionophore ionomycin singly promoted a 25% increase ($P < 0.05$; $n = 3$) in [^{3}H]thymidine incorporation and when combined with PDB gave an additive effect in inducing [^{3}H]thymidine incorporation equal to that induced by AVP. To further substantiate the role of Ca^{2+} in DNA synthesis, we also examined the effect of the Ca^{2+}-chelating agent BAPTA on DNA synthesis. As shown in Fig. 8*D*, pretreatment of cells with 10 μM BAPTA markedly attenuated [^{3}H]thymidine incorporation in response to AVP stimulation. Together, these results suggest that PKC activation and Ca^{2+} mobilization play important roles in mediating DNA synthesis in response to AVP.

To determine whether Src family kinases are also involved in AVP-induced DNA synthesis, cultures of IEC-18 cells were pretreated with the Src kinase inhibitor PP-2, vehicle, or PP-3, a biologically inactive analog of PP2, and then incubated in the absence or the presence of AVP. As illustrated in Fig. 9*A*, exposure to PP-2 prevented AVP-induced [^{3}H]thymidine incorporation in a dose-dependent manner, with complete inhibition achieved at 10 μM. In contrast, addition of PP-3 (also at 10 μM) had no effect on DNA synthesis stimulated by AVP.

Our results indicating that EGFR tyrosine kinase activity is required for AVP-induced ERK-1/2 phosphorylation (Fig. 6*C*) prompted us to examine whether EGFR is also involved in AVP-induced DNA synthesis. Serum-deprived cultures of IEC-18 cells were preincubated for 1 h with the selective EGFR tyrosine kinase inhibitor tyrphostin AG-1478 at various concentrations (31–500 nM) before stimulation with AVP. As shown in Fig. 9*B*, tyrphostin AG-1478 markedly reduced [^{3}H]thymidine incorporation in response to AVP stimulation in a concentration-dependent fashion. Maximal inhibitory effect (~60%) was achieved at a tyrphostin AG-1478 concentration of 100 nM. Together, the results presented in Figs. 8 and 9 indicate that the activity of the ERKs, PKCs, Src family kinases, and EGFR tyrosine kinase and elevation in $[Ca^{2+}]_i$ are required for AVP-induced mitogenesis in IEC-18 cells.

AVP-induced cell migration is dependent on MEK, PKC, and Src family kinase activity. Having established that AVP can act as a potent growth factor in IEC-18 cells, stimulating DNA synthesis and cell proliferation, we next examined whether AVP can also promote cell migration of these cells into a denuded area. Cells were plated on glass coverslips and serum-starved overnight before wounding as described in MATERIALS AND METHODS. The "wounded" coverslips were then incubated in serum-free DMEM supplemented with or without various concentrations of AVP. As shown in Fig. 10*A*, AVP induced a dose-dependent increase in migrating cells into the wound when assessed at 24 h. Pretreatment of the cell cultures with the selective V_{1A} receptor antagonist completely abolished AVP-induced increase in cell migration (Fig. 10*B*).

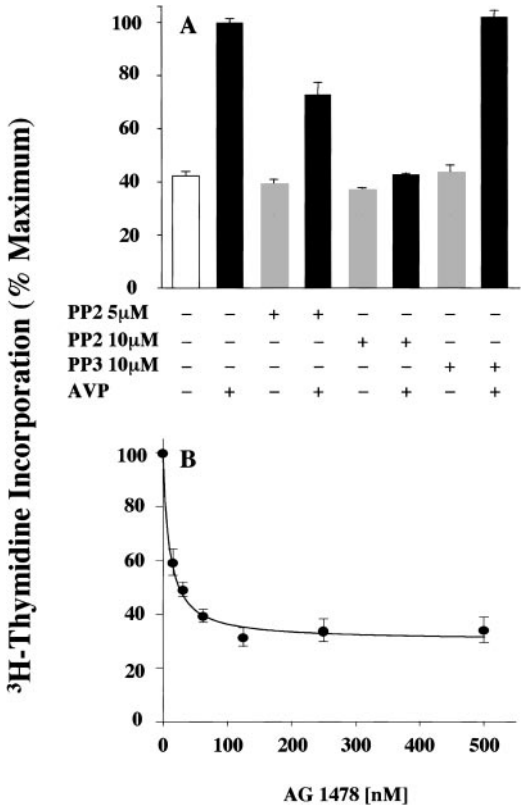

Fig. 9. Effect of inhibitors of Src family kinases and EGFR tyrosine kinase on AVP-induced DNA synthesis. *A*: effect of the Src family kinase activity inhibitor PP-2 on DNA synthesis in response to AVP. Confluent quiescent cultures of IEC-18 cells were washed and incubated at 37°C in 2 ml of DMEM-Waymouth's medium containing 50 nM AVP without or with PP-2 at 5 or 10 μM as indicated. Control cells (−) received equivalent amount of solvent or 10 μM PP-3, a biologically inactive analog of PP-2, and [^{3}H]thymidine incorporation into acid-precipitable material was measured. Results are expressed as mean ± SE % of the maximum increase ($n = 3$) obtained with 50 nM AVP. *B*: tyrphostin AG-1478 inhibits AVP-induced DNA synthesis in a concentration-dependent manner. Confluent quiescent cultures of IEC-18 cells were washed and incubated at 37°C in 2 ml of DMEM-Waymouth's medium containing 50 nM AVP without or with AG-1478 at various concentrations as indicated, and [^{3}H]thymidine incorporation into acid-precipitable material was measured. Results are expressed as mean ± SE % of the maximum increase ($n = 3$) obtained with 50 nM AVP after subtraction of the basal [^{3}H]thymidine incorporation from the respective controls.

Multiple signaling pathways have been implicated in the regulation of cell migration, including ERK (11), PKC (54), and Src (19). In the present study, we examined whether these pathways are also implicated in AVP-induced migration of IEC-18 cells. As shown in Fig. 10*C*, pretreatment with specific MEK inhibitors PD-98059 or the structurally unrelated compound

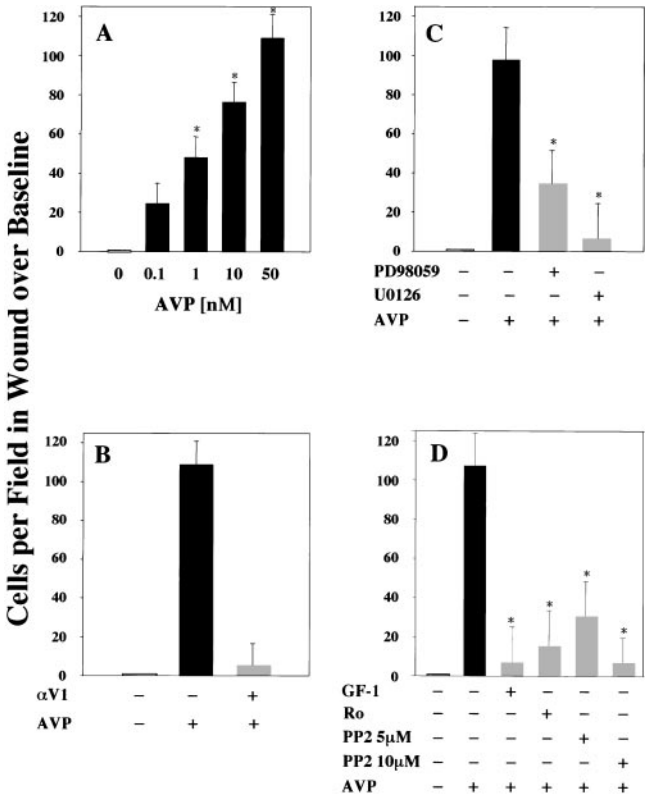

Fig. 10. AVP-induced cell migration is dependent on MEK, PKC, and Src-family kinase activity. *A*: AVP induces cell migration in a dose-dependent manner. Cell monolayers were "wounded" as described in MATERIALS AND METHODS and then placed in serum-free medium in the presence or absence of various concentrations of AVP. $*P < 0.05$ vs. control. *B*: AVP-stimulated cell migration is prevented by exposure to the selective V_{1A} receptor antagonist αV_1. IEC-18 cell monolayers were preincubated with αV_1 (50 nM) before addition of 50 nM AVP. *C*: MEK inhibitors attenuated AVP-stimulated cell migration. IEC-18 cell monolayers were preincubated with 10 μM PD-98059 or 2.5 μM U-0126. Control cells received equivalent amount of solvent (−). The monolayers were subsequently unstimulated (−) or stimulated (+) with 50 nM AVP. $*P < 0.05$ vs. 50 nM AVP. *D*: inhibitors of PKC and Src-kinase abrogate AVP-stimulated cell migration. IEC-18 cell monolayers were preincubated with 2.5 μM GF-I, 2.5 μM Ro-31-8220, 5 μM PP-2, or 10 μM PP-2 before stimulation with 50 nM AVP. Control cells received equivalent amount of solvent (−). Results are mean ± SE number of cells migrated into the denuded area after subtraction of the basal number of cells migrating into the wound seen in controls. $*P < 0.05$ vs. 50 nM AVP.

U-0126 dramatically reduced AVP-induced cell migration.

Similarly, pretreatment with selective PKC inhibitors GF-I and Ro-31-8220 markedly reduced AVP-induced cell migration (Fig. 10*D*). Furthermore, exposure to the Src kinase inhibitor PP-2 prevented AVP-induced cell migration in a dose-dependent manner, with near-complete inhibition achieved at 10 μM. (Fig. 10*D*). These findings demonstrate that AVP induces migration of IEC-18 cells through ERK-, PKC-, and Src-dependent pathways and thus identify signaling pathways that lead to both cell migration and proliferation.

DISCUSSION

The proliferation of epithelial cells of the intestinal mucosa is a tightly regulated process that is modulated by a broad spectrum of regulatory peptides (8, 36, 70). Nontransformed IEC-6 and IEC-18 cells, derived from rat small intestinal crypt (56), have provided an in vitro model to examine intestinal epithelial cell migration, differentiation, and proliferation (16, 27, 58, 70). However, the signal transduction pathways involved in intestinal epithelial cell proliferation have remained incompletely understood. In particular, little was known about the regulation of intestinal cell proliferation in response to GPCR agonists.

In the present study we demonstrate for the first time that addition of the neurohypophysial nonapeptide AVP to cultures of IEC-18 cells potently stimulates multiple intracellular signal transduction pathways. Our results demonstrate that AVP, acting through the V_{1A} receptor subtype, induces a rapid and transient increase in $[Ca^{2+}]_i$ and stimulates a striking increase in PKD activity through a PKC-dependent signal transduction pathway in IEC-18 cells. We recently reported (10) that angiotensin and LPA also induce PKC-dependent PKD activation in IEC-6 and IEC-18 cells. Together, these results support the hypothesis that PKD is a downstream target of PKC in intestinal epithelial cells.

Pyk2, a nonreceptor tyrosine kinase, is stimulated by transient increases in the cytoplasmic concentration of Ca^{2+} and by activation of PKCs in a variety of cell types (41, 42, 72). This enzyme is the second member of the FAK subfamily that localizes to focal adhesions (72) and is expressed in the epithelial cells of the intestine, as shown by immunohistochemical staining and in situ hybridization (48). In the present study, we found that AVP induces rapid Pyk2 tyrosine phosphorylation (indicative of Pyk2 activation) in a concentration-dependent fashion. The phosphorylation of Pyk2 at Tyr^{402}, the major autophosphorylation site, creates a potential high-affinity binding site for the SH2 domain of Src, leading to the formation of a Pyk2-Src signaling complex in which both kinases are thought to be active. The increase in the activity of Src in intact cells can be detected by monitoring the phosphorylation of Src at Tyr^{418}, a phosphorylation site located in its kinase activation loop. Here, we found that AVP induces phosphorylation of Pyk2 at Tyr^{402} and promotes a rapid and striking increase in the phosphorylation of Src at Tyr^{418}, indicating that AVP induces Src family kinase activation in IEC-18 cells.

The MAPKs are a family of highly conserved serine/threonine kinases that are activated by a range of extracellular signals via protein phosphorylation cascades (59) that relay mitogenic signals to the nucleus (39), thereby modulating the activity of transcription factors (79). The two best characterized isoforms, $p42^{mapk}$ (ERK-2) and $p44^{mapk}$ (ERK-1), are directly activated by phosphorylation on specific tyrosine and threonine residues by the dual-specificity ERK kinase (or MEK) (73). Pyk2 and Src have been identified as

upstream kinases leading to the activation of the Raf-MEK-ERK cascade (15, 18, 30, 66). Here, we show that addition of AVP to IEC-18 cells stimulates MEK-dependent ERK activation. Furthermore, we have established that AVP-induced ERK activation is PKC dependent, suggesting that PKC is a critical kinase that lies upstream of MEK/ERK.

There is increasing evidence that tyrosine kinases are involved in the stimulation of the ERK phosphorylation cascade by GPCR agonists. The EGFR is a single-pass transmembrane tyrosine kinase that is activated by direct binding of at least six EGF-related ligands that are synthesized as transmembrane precursors (9, 31). Recently, it was shown that a variety of GPCR agonists also induce a rapid increase in EGFR tyrosine autophosphorylation in several cell types (12–14, 37, 80), a receptor crosstalk termed transactivation (9, 55). Recently, Keely et al. (37) demonstrated that inhibition of EGFR tyrosine kinase activity prevented ERK activation in response to stimulation of G_q-coupled muscarinic M_3 receptor by carbachol in colonic epithelial cells. EGFR transactivation is thought to induce ERK activation via a well-defined mechanism involving SOS-Grb2-mediated accumulation of Ras-GTP, which then recruits Raf-1 to the plasma membrane and activates a kinase cascade comprising Raf, MEK, and the ERKs (46, 73). In our study, we demonstrated that inhibition of EGFR tyrosine kinase activity prevented ERK activation in response to AVP. Moreover, treatment of IEC-18 cells with the selective Src kinase inhibitor PP-2 completely prevented ERK activation in response to AVP stimulation. Thus AVP induces ERK activation through $[Ca^{2+}]_i$, PKCs, EGFR tyrosine kinase, and Src family kinases in IEC-18 cells.

The requirement of these upstream pathways for ERK activation together with our kinetic results could be explained in the framework of a model in which $[Ca^{2+}]_i$ and PKC are required for Pyk2 activation, leading to Tyr^{402} phosphorylation (Fig. 4*C*). This site of Pyk2 associates with and leads to activation of Src family members (Fig. 4*D*). In line with this model, our results show a striking similarity between the time courses of Pyk2 tyrosine phosphorylation and Src activation (Fig. 4, *B* and *D*). Interestingly, Pyk2 and Src were implicated in promoting EGFR transactivation (4, 38). The fact that these tyrosine phosphorylation pathways are upstream of ERK is further supported by our kinetic results demonstrating that the rapid activation of Pyk2 and Src preceded ERK activation (Fig. 4*E*). Although the confirmation of this signal transduction model will require further experimental work, it provides a plausible explanation for the requirement of $[Ca^{2+}]_i$, PKC, EGFR, and Src for ERK activation in AVP-stimulated intestinal epithelial cells.

Our results demonstrate that AVP initiates multiple early signaling pathways in IEC-18 cells that are increasingly implicated in stimulating cell proliferation. Indeed, one of the most interesting findings presented in this study is that addition of AVP to cultures of IEC-18 cells induces DNA synthesis and cell proliferation in the absence of any other exogenously added growth factor and at nanomolar concentrations. AVP was more effective than EGF in stimulating [^{3}H]thymidine incorporation in IEC-18 cells. These findings indicate that, in addition to tyrosine kinase receptors, GPCRs are also involved in the regulation of cell proliferation of intestinal epithelial cells.

Using selective inhibitors of MEK-mediated ERK activation, Src family kinase activity, and EGFR tyrosine kinase activity, we found that ERK inhibition attenuated AVP-induced DNA synthesis whereas either Src or EGFR inhibition markedly diminished this response. Because our results indicate that Src and EGFR are upstream of ERK in the pathway triggered by AVP in IEC-18 cells, it is conceivable that, in addition to ERK, Src kinases and EGFR are involved in triggering additional signaling pathways leading to DNA synthesis induced by AVP in these cells. We conclude that AVP is a potent growth factor for IEC-18 cells and that Src and EGFR play critical roles in mediating the proliferative response elicited by AVP in these cells.

The PKC family has been implicated in the signal transduction pathways that mediate important functions in intestinal epithelial cells including proliferation (1, 22) and carcinogenesis (53). It is known that intestinal epithelial cells express multiple isoforms of the PKC family, including α, β, δ, ϵ, and ζ. Mice with transgenic overexpression of PKCβ2 in the intestinal epithelium exhibit hyperproliferation of the colonic epithelium and an increased susceptibility to azoxymethane-induced preneoplastic lesions in the colon (49). PKCϵ has been shown to act as an oncogene when overexpressed in intestinal epithelial cells (53). PKC has also been implicated in the downregulation of the tumor suppressor gene *Cdx-2* by oncogenic Ras in vivo (45). In actively cycling IEC-18 cells (cells growing in 5% serum), treatment with biologically active phorbol esters transiently inhibited cell cycle progression, which was noted 2–6 h after treatment (22, 23). This cell cycle delay was associated with a rapid decrease in the level of cyclin D1, which subsequently rebounded and, in fact, increased over the basal levels at later times of phorbol ester treatment (23).

The results presented here demonstrate that exposure of quiescent, serum-starved IEC-18 cells to PDB stimulated an increase in DNA synthesis at a time that coincided with cyclin D1 elevation noted in a previous study (Fig. 8*C*; Ref. 23). Furthermore, treatment with selective PKC inhibitors abolished ERK activation and markedly attenuated DNA synthesis in response to AVP. These results suggest that PKC could play different roles in cell proliferation at different stages of the cell cycle (44). Collectively, our results indicate that receptor-mediated PKC activation, as induced by AVP, transduces mitogenic signals leading to DNA synthesis and cell proliferation in IEC-18 cells.

In the gastrointestinal mucosa, cell proliferation and migration play a fundamental role in the organization and maintenance of tissue integrity (50). When damaged, the gastrointestinal mucosa has a remarkable ability to repair itself very rapidly. Within minutes of

epithelial injury, cells adjacent to a wound rapidly migrate over the denuded area to reestablish epithelial continuity. Subsequently, the cells enter into DNA synthesis and divide. This two-stage process of wound repair is known as restitution. Cultures of IEC cells have provided an excellent model system to study restitution in cell culture (16, 27, 58, 70). In addition to DNA synthesis and cell proliferation, we have shown that AVP via V_{1A} receptor promotes cell migration in cultures of IEC-18 cells in a dose-dependent manner and is dependent on MEK, PKC, and Src family kinase activity. Interestingly, like many other neuropeptides, AVP production and release is not restricted to the hypothalamic neurohypophysial system. Indeed, AVP immunoreactivity and AVP-associated neurophysin were localized to crypt cells of rodent and human small intestine, suggesting that in addition to its well-known role as an endocrine hormone produced by hypothalamic neurons, AVP can also act as a paracrine signaling peptide in the intestine (24, 25, 69).

Thus the findings presented in this study raise the possibility that AVP plays a role in the maintenance of the intestinal mucosa in response to injury by promoting intestinal epithelial cell proliferation and migration.

We thank Dr. Doreen Cantrell (Imperial Cancer Research Fund, London, UK) for the generous gift of phosphoserine 916 antibody and Nena Hsieh for technical assistance.

This work was supported by National Institute of Diabetes and Digestive and Kidney Diseases Grants DK-55003 and DK-56930 to E. Rozengurt. T. Chiu is a recipient of an American Gastroenterological Association (AGA)-AstraZeneca Fellowship/Faculty Transition Award. S. S. Wu is a National Institutes of Health Fellow of the Pediatric Scientist Development Program (K12-HD-00850).

REFERENCES

1. **Abraham C, Scaglione-Sewell B, Skarosi SF, Qin W, Bissonnette M, and Brasitus TA.** Protein kinase C alpha modulates growth and differentiation in Caco-2 cells. *Gastroenterology* 114: 503–509, 1998.
2. **Abram CL and Courtneidge SA.** Src family tyrosine kinases and growth factor signaling. *Exp Cell Res* 254: 1–13, 2000.
3. **Andrâe F, Rigot V, Remacle-Bonnet M, Luis J, Pommier G, and Marvaldi J.** Protein kinases C-gamma and -delta are involved in insulin-like growth factor I-induced migration of colonic epithelial cells. *Gastroenterology* 116: 64–77, 1999.
4. **Andreev J, Galisteo ML, Kranenburg O, Logan SK, Chiu ES, Okigaki M, Cary LA, Moolenaar WH, and Schlessinger J.** Src and Pyk2 mediate G-protein-coupled receptor activation of epidermal growth factor receptor (EGFR) but are not required for coupling to the mitogen-activated protein (MAP) kinase signaling cascade. *J Biol Chem* 276: 20130–20135, 2001.
5. **Berridge MJ.** Inositol trisphosphate and calcium signalling. *Nature* 361: 315–325, 1993.
6. **Birnbaumer M.** Vasopressin receptors. *Trends Endocrinol Metab* 11: 406–410, 2000.
7. **Bridges AJ, Zhou H, Cody DR, Rewcastle GW, McMichael A, Showalter HD, Fry DW, Kraker AJ, and Denny WA.** Tyrosine kinase inhibitors. An unusually steep structure-activity relationship for analogues of 4-(3-bromoanilino)-6,7-dimethoxyquinazoline (PD 153035), a potent inhibitor of the epidermal growth factor receptor. *J Med Chem* 39: 267–276, 1996.
8. **Burgess AW.** Growth control mechanisms in normal and transformed intestinal cells. *Philos Trans R Soc Lond B Biol Sci* 353: 903–909, 1998.
9. **Carpenter G.** Employment of the epidermal growth factor receptor in growth factor-independent signaling pathways. *J Cell Biol* 146: 697–702, 1999.
10. **Chiu T and Rozengurt E.** PKD in intestinal epithelial cells: rapid activation by phorbol esters, LPA, and angiotensin through PKC. *Am J Physiol Cell Physiol* 280: C929–C942, 2001.
11. **Cho SY and Klemke RL.** Extracellular-regulated kinase activation and CAS/Crk coupling regulate cell migration and suppress apoptosis during invasion of the extracellular matrix. *J Cell Biol* 149: 223–236, 2000.
12. **Cunnick JM, Dorsey JF, Standley T, Turkson J, Kraker AJ, Fry DW, Jove R, and Wu J.** Role of tyrosine kinase activity of epidermal growth factor receptor in the lysophosphatidic acid-stimulated mitogen-activated protein kinase pathway. *J Biol Chem* 273: 14468–14475, 1998.
13. **Daub H, Weiss FU, Wallasch C, and Ullrich A.** Role of transactivation of the EGF receptor in signalling by G-protein-coupled receptors. *Nature* 379: 557–560, 1996.
14. **Daub H, Wallasch C, Lankenau A, Herrlich A, and Ullrich A.** Signal characteristics of G protein-transactivated EGF receptor. *EMBO J* 16: 7032–7044, 1997.
15. **Della Rocca GJ, van Biesen T, Daaka Y, Luttrell DK, Luttrell LM, and Lefkowitz RJ.** Ras-dependent mitogen-activated protein kinase activation by G protein-coupled receptors. Convergence of G_i- and G_q-mediated pathways on calcium/calmodulin, Pyk2, and Src kinase. *J Biol Chem* 272: 19125–19132, 1997.
16. **Dignass AU and Podolsky DK.** Cytokine modulation of intestinal epithelial cell restitution: central role of transforming growth factor beta. *Gastroenterology* 105: 1323–1332, 1993.
17. **Dignass AU, Tsunekawa S, and Podolsky DK.** Fibroblast growth factors modulate intestinal epithelial cell growth and migration. *Gastroenterology* 106: 1254–1262, 1994.
18. **Dikic I, Tokiwa G, Lev S, Courtneidge SA, and Schlessinger J.** A role for Pyk2 and Src in linking G-protein-coupled receptors with MAP kinase activation. *Nature* 383: 547–550, 1996.
19. **Emami S, Le Floch N, Bruyneel E, Thim L, May F, Westley B, Rio MC, Mareel M, and Gespach C.** Induction of scattering and cellular invasion by trefoil peptides in src- and RhoA-transformed kidney and colonic epithelial cells. *FASEB J* 15: 351–361, 2001.
20. **Exton JH.** Regulation of phosphoinositide phospholipases by hormones, neurotransmitters, and other agonists linked to G proteins. *Annu Rev Pharmacol Toxicol* 36: 481–509, 1996.
21. **Favata MF, Horiuchi KY, Manos EJ, Daulerio AJ, Stradley DA, Feeser WS, Van Dyk DE, Pitts WJ, Earl RA, Hobbs F, Copeland RA, Magolda RL, Scherle PA, and Trzaskos JM.** Identification of a novel inhibitor of mitogen-activated protein kinase kinase. *J Biol Chem* 273: 18623–18632, 1998.
22. **Frey MR, Saxon ML, Zhao X, Rollins A, Evans SS, and Black JD.** Protein kinase C isozyme-mediated cell cycle arrest involves induction of p21(waf1/cip1) and p27(kip1) and hypophosphorylation of the retinoblastoma protein in intestinal epithelial cells. *J Biol Chem* 272: 9424–9435, 1997.
23. **Frey MR, Clark JA, Leontieva O, Uronis JM, Black AR, and Black JD.** Protein kinase C signaling mediates a program of cell cycle withdrawal in the intestinal epithelium. *J Cell Biol* 151: 763–777, 2000.
24. **Friedmann A, Memoli V, and North W.** Evidence for vasopressin production in the human gastrointestinal system. *Peptides* 12: 1051–1056, 1991.
25. **Friedmann A, Memoli V, Yu X, and North W.** Biosynthesis of vasopressin by gastrointestinal cells of Brattleboro and Long-Evans rats. *Peptides* 14: 607–612, 1993.
26. **Fry DW, Kraker AJ, McMichael A, Ambroso LA, Nelson JM, Leopold WR, Connors RW, and Bridges AJ.** A specific inhibitor of the epidermal growth factor receptor tyrosine kinase. *Science* 265: 1093–1095, 1994.
27. **Gèoke M, Kanai M, and Podolsky DK.** Intestinal fibroblasts regulate intestinal epithelial cell proliferation via hepatocyte growth factor. *Am J Physiol Gastrointest Liver Physiol* 274: G809–G818, 1998.

28. **Granot Y, Erikson E, Fridman H, Van Putten V, Williams B, Schrier RW, and Maller JL.** Direct evidence for tyrosine and threonine phosphorylation and activation of mitogen-activated protein kinase by vasopressin in cultured rat vascular smooth muscle cells. *J Biol Chem* 268: 9564–9569, 1993.
29. **Grynkiewicz G, Poenie M, and Tsien RY.** A new generation of Ca^{2+} indicators with greatly improved fluorescence properties. *J Biol Chem* 260: 3440–3450, 1985.
30. **Gutkind JS.** The pathways connecting G protein-coupled receptors to the nucleus through divergent mitogen-activated protein kinase cascades. *J Biol Chem* 273: 1839–1842, 1998.
31. **Hackel PO, Zwick E, Prenzel N, and Ullrich A.** Epidermal growth factor receptors: critical mediators of multiple receptor pathways. *Curr Opin Cell Biol* 11: 184–189, 1999.
32. **Hamilton M and Wolfman A.** Oncogenic Ha-ras-dependent mitogen-activated protein kinase activity requires signaling through the epidermal growth factor receptor. *J Biol Chem* 273: 28155–28162, 1998.
33. **Hanke JH, Gardner JP, Dow RL, Changelian PS, Brissette WH, Weringer EJ, Pollok BA, and Connelly PA.** Discovery of a novel, potent, and Src family-selective tyrosine kinase inhibitor. Study of Lck- and FynT-dependent T cell activation. *J Biol Chem* 271: 695–701, 1996.
34. **Hayashi A, Seki N, Hattori A, Kozuma S, and Saito T.** PKCnu, a new member of the protein kinase C family, composes a fourth subfamily with PKCmu. *Biochim Biophys Acta* 1450: 99–106, 1999.
35. **Hervieu G, Volant K, Grishina O, Descroix-Vagne M, and Nahon JL.** Similarities in cellular expression and functions of melanin-concentrating hormone and atrial natriuretic factor in the rat digestive tract. *Endocrinology* 137: 561–571, 1996.
36. **Kanai M, Mullen C, and Podolsky DK.** Intestinal trefoil factor induces inactivation of extracellular signal-regulated protein kinase in intestinal epithelial cells. *Proc Natl Acad Sci USA* 95: 178–182, 1998.
37. **Keely SJ, Uribe JM, and Barrett KE.** Carbachol stimulates transactivation of epidermal growth factor receptor and mitogen-activated protein kinase in T84 cells. Implications for carbachol-stimulated chloride secretion. *J Biol Chem* 273: 27111–27117, 1998.
38. **Keely SJ, Calandrella SO, and Barrett KE.** Carbachol-stimulated transactivation of epidermal growth factor receptor and mitogen-activated protein kinase in T84 cells is mediated by intracellular Ca^{2+}, PYK-2, and p60src. *J Biol Chem* 275: 12619–12625, 2000.
39. **Khokhlatchev AV, Canagarajah B, Wilsbacher J, Robinson M, Atkinson M, Goldsmith E, and Cobb MH.** Phosphorylation of the MAP kinase ERK2 promotes its homodimerization and nuclear translocation. *Cell* 93: 605–615, 1998.
40. **Kruszynski M, Lammek B, Manning M, Seto J, Haldar J, and Sawyer WH.** [1-beta-Mercapto-beta,beta-cyclopentamethylenepropionic acid,2-(*O*-methyl)tyrosine] arginine-vasopressin and [1-beta-mercapto-beta,beta-cyclopentamethylenepropionic acid] arginine-vasopressin, two highly potent antagonists of the vasopressor response to arginine-vasopressin. *J Med Chem* 23: 364–368, 1980.
41. **Lev S, Moreno H, Martinez R, Canoll P, Peles E, Musacchio JM, Plowman GD, Rudy B, and Schlessinger J.** Protein tyrosine kinase PYK2 involved in Ca^{2+}-induced regulation of ion channel and MAP kinase functions. *Nature* 376: 737–745, 1995.
42. **Li LX and Earp HS.** Paxillin is tyrosine-phosphorylated by and preferentially associates with the calcium-dependent tyrosine kinase in rat liver epithelial cells. *J Biol Chem* 272: 14341–14348, 1997.
43. **Lipson KE, Pang L, Huber LJ, Chen H, Tsai JM, Hirth P, Gazit A, Levitzki A, and McMahon G.** Inhibition of platelet-derived growth factor and epidermal growth factor receptor signaling events after treatment of cells with specific synthetic inhibitors of tyrosine kinase phosphorylation. *J Pharmacol Exp Ther* 285: 844–852, 1998.
44. **Livneh E and Fishman DD.** Linking protein kinase C to cell-cycle control. *Eur J Biochem* 248: 1–9, 1997.
45. **Lorentz O, Cadoret A, Duluc I, Capeau J, Gespach C, Cherqui G, and Freund JN.** Downregulation of the colon tumour-suppressor homeobox gene Cdx-2 by oncogenic ras. *Oncogene* 18: 87–92, 1999.
46. **Marshall CJ.** Specificity of receptor tyrosine kinase signaling: transient versus sustained extracellular signal-regulated kinase activation. *Cell* 80: 179–185, 1995.
47. **Matthews SA, Rozengurt E, and Cantrell D.** Characterization of serine 916 as an in vivo autophosphorylation site for protein kinase D/protein kinase C mu. *J Biol Chem* 274: 26543–26549, 1999.
48. **Mitaka T, Shindoh M, Mochizuki Y, Sasaki H, Ishino M, Matsuya M, Ninomiya T, and Sasaki T.** Restricted expression of cell adhesion kinase-beta in rat tissues. *Am J Pathol* 150: 267–281, 1997.
49. **Murray NR, Davidson LA, Chapkin RS, Clay Gustafson W, Schattenberg DG, and Fields AP.** Overexpression of protein kinase C betaII induces colonic hyperproliferation and increased sensitivity to colon carcinogenesis. *J Cell Biol* 145: 699–711, 1999.
50. **Nusrat A, Delp C, and Madara JL.** Intestinal epithelial restitution. Characterization of a cell culture model and mapping of cytoskeletal elements in migrating cells. *J Clin Invest* 89: 1501–1511, 1992.
51. **Nusrat A, Parkos CA, Bacarra AE, Godowski PJ, Delp-Archer C, Rosen EM, and Madara JL.** Hepatocyte growth factor/scatter factor effects on epithelia. Regulation of intercellular junctions in transformed and nontransformed cell lines, basolateral polarization of c-met receptor in transformed and natural intestinal epithelia, and induction of rapid wound repair in a transformed model epithelium. *J Clin Invest* 93: 2056–2065, 1994.
52. **Okada T, Sakuma L, Fukui Y, Hazeki O, and Ui M.** Blockage of chemotactic peptide-induced stimulation of neutrophils by wortmannin as a result of selective inhibition of phosphatidylinositol 3-kinase. *J Biol Chem* 269: 3563–3567, 1994.
53. **Perletti GP, Marras E, Concari P, Piccinini F, and Tashjian AH Jr.** PKCdelta acts as a growth and tumor suppressor in rat colonic epithelial cells. *Oncogene* 18: 1251–1256, 1999.
54. **Polk DB.** Epidermal growth factor receptor-stimulated intestinal epithelial cell migration requires phospholipase C activity. *Gastroenterology* 114: 493–502, 1998.
55. **Prenzel N, Zwick E, Daub H, Leserer M, Abraham R, Wallasch C, and Ullrich A.** EGF receptor transactivation by G-protein-coupled receptors requires metalloproteinase cleavage of proHB-EGF. *Nature* 402: 884–888, 1999.
56. **Quaroni A, Wands J, Trelstad RL, and Isselbacher KJ.** Epithelioid cell cultures from rat small intestine. Characterization by morphologic and immunologic criteria. *J Cell Biol* 80: 248–265, 1979.
57. **Quaroni A and May RJ.** Establishment and characterization of intestinal epithelial cell cultures. *Methods Cell Biol* 21B: 403–427, 1980.
58. **Ray RM, Zimmerman BJ, McCormack SA, Patel TB, and Johnson LR.** Polyamine depletion arrests cell cycle and induces inhibitors p21(Waf1/Cip1), p27(Kip1), and p53 in IEC-6 cells. *Am J Physiol Cell Physiol* 276: C684–C691, 1999.
59. **Robinson MJ and Cobb MH.** Mitogen-activated protein kinase pathways. *Curr Opin Cell Biol* 9: 180–186, 1997.
60. **Rodríguez-Fernández JL and Rozengurt E.** Bombesin, bradykinin, vasopressin, and phorbol esters rapidly and transiently activate Src family tyrosine kinases in Swiss 3T3 cells. Dissociation from tyrosine phosphorylation of p125 focal adhesion kinase. *J Biol Chem* 271: 27895–27901, 1996.
61. **Rodríguez-Fernández JL and Rozengurt E.** Bombesin, vasopressin, lysophosphatidic acid, and sphingosylphosphorylcholine induce focal adhesion kinase activation in intact Swiss 3T3 cells. *J Biol Chem* 273: 19321–19328, 1998.
62. **Rozengurt E, Legg A, and Pettican P.** Vasopressin stimulation of mouse 3T3 cell growth. *Proc Natl Acad Sci USA* 76: 1284–1287, 1979.
63. **Rozengurt E.** Early signals in the mitogenic response. *Science* 234: 161–166, 1986.

64. **Rozengurt E.** Neuropeptides as cellular growth factors: role of multiple signalling pathways. *Eur J Clin Invest* 21: 123–134, 1991.
65. **Rozengurt E, Sinnett-Smith J, and Zugaza JL.** Protein kinase D: a novel target for diacylglycerol and phorbol esters. *Biochem Soc Trans* 25: 565–571, 1997.
66. **Rozengurt E.** Signal transduction pathways in the mitogenic response to G protein-coupled neuropeptide receptor agonists. *J Cell Physiol* 177: 507–517, 1998.
67. **Rozengurt E and Walsh JH.** Gastrin, CCK, signaling and cancer. *Annu Rev Physiol* 63: 49–76, 2001.
68. **Russell WE and Bucher NL.** Vasopressin modulates liver regeneration in the Brattleboro rat. *Am J Physiol Gastrointest Liver Physiol* 245: G321–G324, 1983.
69. **Sánchez-Franco F, Cacicedo L, Vasallo JL, Blazquez JL, and Muñoz Barragan L.** Arginine-vasopressin immunoreactive material in the gastrointestinal tract. *Histochemistry* 85: 419–422, 1986.
70. **Santos MF, McCormack SA, Guo Z, Okolicany J, Zheng Y, Johnson LR, and Tigyi G.** Rho proteins play a critical role in cell migration during the early phase of mucosal restitution. *J Clin Invest* 100: 216–225, 1997.
71. **Sato Y, Hanai H, Nogaki A, Hirasawa K, Kaneko E, Hayashi H, and Suzuki Y.** Role of the vasopressin V_1 receptor in regulating the epithelial functions of the guinea pig distal colon. *Am J Physiol Gastrointest Liver Physiol* 277: G819–G828, 1999.
72. **Schaller MD and Sasaki T.** Differential signaling by the focal adhesion kinase and cell adhesion kinase beta. *J Biol Chem* 272: 25319–25325, 1997.
73. **Seger R and Krebs EG.** The MAPK signaling cascade. *FASEB J* 9: 726–735, 1995.
74. **Sethi T and Rozengurt E.** Multiple neuropeptides stimulate clonal growth of small cell lung cancer: effects of bradykinin, vasopressin, cholecystokinin, galanin, and neurotensin. *Cancer Res* 51: 3621–3623, 1991.
75. **Sturany S, Van Lint J, Mueller F, Wilda M, Hameister H, Hoecker M, Brey A, Gern U, Vandenheede J, Gress T, Adler G, and Seufferlein T.** Molecular cloning and characterization of the human protein kinase D2: a novel member of the protein kinase D family of serine threonine kinases. *J Biol Chem* 276: 3310–3318, 2001.
76. **Tangkijvanich P, Tam SP, and Yee HF.** Wound-induced migration of rat hepatic stellate cells is modulated by endothelin-1 through rho-kinase-mediated alterations in the acto-myosin cytoskeleton. *Hepatology* 33: 74–80, 2001.
77. **Thibonnier M, Conarty DM, and Plesnicher CL.** Mediators of the mitogenic action of human V_1 vascular vasopressin receptors. *Am J Physiol Heart Circ Physiol* 279: H2529–H2539, 2000.
78. **Toullec D, Pianetti P, Coste H, Bellevergue P, Grandperret T, Ajakane M, Baudet V, Boissin P, Boursier E, Loriolle F, Duhamel L, Charon D, and Kirilovsky J.** The bisindolylmaleimide GF-109203x is a potent and selective inhibitor of protein kinase-C. *J Biol Chem* 266: 15771–15781, 1991.
79. **Treisman R.** Regulation of transcription by MAP kinase cascades. *Curr Opin Cell Biol* 8: 205–215, 1996.
80. **Tsai W, Morielli AD, and Peralta EG.** The m1 muscarinic acetylcholine receptor transactivates the EGF receptor to modulate ion channel activity. *EMBO J* 16: 4597–4605, 1997.
81. **Van Lint JV, Sinnett-Smith J, and Rozengurt E.** Expression and characterization of PKD, a phorbol ester and diacylglycerol-stimulated serine protein kinase. *J Biol Chem* 270: 1455–1461, 1995.
82. **Ward SM, Bayguinov OP, Lee HK, and Sanders KM.** Excitatory and inhibitory actions of vasopressin on colonic excitation-contraction coupling in dogs. *Gastroenterology* 113: 1233–1245, 1997.
83. **Widmann C, Gibson S, Jarpe MB, and Johnson GL.** Mitogen-activated protein kinase: conservation of a three-kinase module from yeast to human. *Physiol Rev* 79: 143–180, 1999.
84. **Yeo EJ and Exton JH.** Stimulation of phospholipase D by epidermal growth factor requires protein kinase C activation in Swiss 3T3 cells. *J Biol Chem* 270: 3980–3988, 1995.
85. **Zugaza JL, Sinnett-Smith J, Van Lint J, and Rozengurt E.** Protein kinase D (PKD) activation in intact cells through a protein kinase C-dependent signal transduction pathway. *EMBO J* 15: 6220–6230, 1996.